Quaternary Science Reviews 296 (2022) 107801

Contents lists available at ScienceDirect

Quaternary Science Reviews

journal homepage: www.elsevier.com/locate/quascirev

Multi-centennial Holocene climate variability in proxy records and transient model simulations

Thomas Gravgaard Askjær [a, b], Qiong Zhang [a, b, *], Frederik Schenk [b, c, d], Fredrik Charpentier Ljungqvist [b, e, f], Zhengyao Lu [g], Chris M. Brierley [h], Peter O. Hopcroft [i], Johann Jungclaus [j], Xiaoxu Shi [k], Gerrit Lohmann [k], Weiyi Sun [l], Jian Liu [l], Pascale Braconnot [m], Bette L. Otto-Bliesner [n], Zhipeng Wu [o, p], Qiuzhen Yin [o], Yibo Kang [q, r], Haijun Yang [q, r]

[a] Department of Physical Geography, Stockholm University, Stockholm, 10691, Sweden
[b] Bolin Centre for Climate Research, Stockholm University, Stockholm, 10691, Sweden
[c] Department of Geological Sciences, Stockholm University, Stockholm, 10691, Sweden
[d] Swedish Meteorological and Hydrological Institute (SMHI), Norrköping, 60176, Sweden
[e] Department of History, Stockholm University, Stockholm, 10691, Sweden
[f] Swedish Collegium for Advanced Study, Uppsala, 75238, Sweden
[g] Department of Physical Geography and Ecosystem Science, Lund University, Lund, 22100, Sweden
[h] Department of Geography, University College London, London, WC1E 6BT, UK
[i] School of Geography, Earth & Environmental Sciences, University of Birmingham, Birmingham, UK
[j] Max Planck Institute for Meteorology, Hamburg, Germany
[k] Alfred Wegener Institute, Helmholtz Centre for Polar and Marine Research, Bremerhaven, Germany
[l] School of Geography Science, Nanjing Normal University, Nanjing, China
[m] Laboratoire des Sciences Du Climat et de l'Environnement, LSCE/IPSL, CEA-CNRS-UVSQ, Université Paris-Saclay, 91191, Gif-sur-Yvette, France
[n] Climate and Global Dynamics Laboratory, National Center for Atmospheric Research (NCAR), Boulder, CO, 80305, USA
[o] George Lemaitre Centre for Earth and Climate Research, Earth and Life Institute, Université catholique de Louvain, Louvain-la-Neuve, Belgium
[p] Key Laboratory of Cenozoic Geology and Environment, Institute of Geology and Geophysics, Chinese Academy of Sciences, Beijing, China
[q] Department of Atmospheric and Oceanic Sciences and Institute of Atmospheric Science and CMA-FDU Joint Laboratory of Marine Meteorology, Fudan University, Shanghai, 200438, China
[r] Shanghai Scientific Frontier Base for Ocean-Atmosphere Interaction Studies, Fudan University, Shanghai, 200438, China

ARTICLE INFO

Article history:
Received 5 August 2022
Received in revised form
24 September 2022
Accepted 25 September 2022
Available online xxx

Handling Editor: C. Hillaire-Marcel

Keywords:
Multi-centennial climate variability
Paleoclimate proxy records
Holocene transient simulations
Spectral analysis
Model-proxy comparison

ABSTRACT

Variability on centennial to multi-centennial timescales is mentioned as a feature in reconstructions of the Holocene climate. As more long transient model simulations with complex climate models become available and efforts have been made to compile large proxy databases, there is now a unique opportunity to study multi-centennial variability with greater detail and a large amount of data than earlier. This paper presents a spectral analysis of transient Holocene simulations from 9 models and 120 proxy records to find the common signals related to oscillation periods and geographic dependencies and discuss the implications for the potential driving mechanisms. Multi-centennial variability is significant in most proxy records, with the dominant oscillation periods around 120–130 years and an average of 240 years. Spectra of model-based global mean temperature (GMT) agree well with proxy evidence with significant multi-centennial variability in all simulations with the dominant oscillation periods around 120–150 years. It indicates a comparatively good agreement between model and proxy data. A lack of latitudinal dependencies in terms of oscillation period is found in both the model and proxy data. However, all model simulations have the highest spectral density distributed over the Northern hemisphere high latitudes, which could indicate a particular variability sensitivity or potential driving mechanisms in this region. Five models also have differentiated forcings simulations with various combinations of forcing agents. Significant multi-centennial variability with oscillation periods between 100 and 200 years is found in all forcing scenarios, including those with only orbital forcing. The different forcings induce some variability in the system. Yet, none appear to be the predominant driver based on

* Corresponding author. Department of Physical Geography, Stockholm University, Stockholm, 10691, Sweden.
E-mail address: qiong.zhang@natgeo.su.se (Q. Zhang).

https://doi.org/10.1016/j.quascirev.2022.107801

the spectral analysis. Solar irradiance has long been hypothesized to be a primary driver of multi-centennial variability. However, all the simulations without this forcing have shown significant multi-centennial variability. The results then indicate that internal mechanisms operate on multi-centennial timescales, and the North Atlantic-Arctic is a region of interest for this aspect.

1. Introduction

In paleoclimate reconstructions, variability on (multi-)centennial time scales is often mentioned as a feature of the climate system, but the details behind it remain elusive and a matter of debate (Andresen et al., 2004a, 2004b; Seppä et al., 2009; Wanner et al., 2011). With the outlook on future climate change, variability on this timescale is of particular interest as the estimated response to anthropogenic forcing is often simulated until 2100 CE, for example, in the Coupled Model Intercomparison Project (CMIP6) (Eyring et al., 2016). Uncertainties in estimations of future climate change are related to both the difficulty of predicting emission scenarios and our understanding of the climate system and, thereby, how well the models can simulate it (Lee et al., 2021). If oscillations on multi-centennial timescales are a significant feature of the climate system, it is essential for future mitigation and adaptation strategies to understand the contribution of natural variability (Lohmann, 2018).

Examining climate variability on multi-centennial timescales requires long and well-resolved time series of paleoclimate data from either proxies or climate models, as even the longest instrumental records are too short. The time series need to be detailed enough to resolve the variability signals and long enough to include several oscillations, which has been a challenge for general circulation models (GCMs) as they require large amounts of computational power to simulate long timespans. Previous studies with proxy-model comparisons of paleoclimate variability using multi-model ensembles from GCMs have been restricted to simulations of the last millennium (Fernández-Donado et al., 2013; Laepple and Huybers, 2014b; Dee et al., 2017; Parsons et al., 2017; Ljungqvist et al., 2019) and only in recent studies have longer transient simulations been used (Zhu et al., 2019; Sun et al., 2022).

Recently, more long Holocene transient simulations are becoming available through the Paleoclimate Modelling Intercomparison Project 4 (PMIP4) (Otto-Bliesner et al., 2017; Kageyama et al., 2018) and other independent works. As a result, there is now an opportunity to study multi-centennial variability (referring to both single century and multi-centennial variability in this work) in greater detail than hitherto possible. In this study, we perform a spectral analysis on temperature in transient Holocene model simulations from 9 different models to test whether they reproduce significant oscillations in the multi-centennial frequency band and if it emerges as a global or regional signal.

As the motivation for examining multi-centennial variability originates from paleoclimate reconstructions, analyzing proxy records alongside the model data is relevant. Therefore, this work will include spectral analysis of 120 proxy records allowing for a model *vs*. proxy comparison of the variability signals.

Proposed driving mechanisms of multi-centennial scale variability have been debated in the scientific literature. Several internal and external drivers have been suggested (Stuiver et al., 1995; Wanner et al., 2008; Marchitto et al., 2010). One external forcing often hypothesized is solar irradiance, as both proxy reconstructions (Beer, 2000; Bond et al., 2001; De Jager, 2005; Asmerom et al., 2007; Usoskin et al., 2016; Wu et al., 2018) and modelling of solar variability (Wilson, 2013) show oscillations close to or coinciding with those from paleoclimate reconstructions. Others suggested internal mechanisms such as the Atlantic Meridional Overturning Circulation (AMOC) (Stuiver et al., 1995; McDermott et al., 2001) and Arctic sea ice (Müller et al., 2012; Hörner et al., 2017) and generally, it is challenging to distinguish between internal variability and externally forced variations (Laepple and Huybers, 2014a). Additional single/differentiated forcing simulations from five models will be analyzed to discuss the potential drivers further.

In summary, this work aims to examine the Holocene climate variability in transient simulations from 9 GCMs to 120 proxy records with an emphasis on the period of the oscillations, regional dependencies and discuss the implications for potential drivers.

2. Material and methods

2.1. Proxy records

The proxy records are collected from the "Arctic Holocene Proxy Climate Database" (AHPC) created by Sundqvist et al. (2014) and the "Temperature 12k Database" (Temp12k) created by Kaufman et al. (2020). From these databases, we select records with a resolution of at least 50 years (except for a few representing glacial parameters). After removing double entries, the proxy ensemble totals 120 records with an average temporal resolution of 28 years, distributed over the climate variables seen in Table 1 in the Appendix.

The proxy records have global coverage with a bias towards the Northern hemisphere (NH) mid-to high-latitudes, under-representation in Siberia, South America and Africa and no records from Australia (see Fig. 1). The details of the individual records are listed in table 4. As this work aims to study multi-centennial variability in the Holocene, the records extending further back than the Holocene have the part older than 10,000 BP excluded from the analysis to avoid mixing up different climate regimes and potentially biasing the results. In the quality control done by Kaufman et al. (2020), a few of the records included in Sundqvist et al. (2014) are commented on concerning uncertainties in age estimations and local factors. These records are marked in table 4 but are still included in the analysis as all except one are still accepted by Kaufman et al. (2020). There are also comments for other records in Kaufman et al. (2020), although the comments do not necessarily provide critique as some just give additional information. For the specific details on the comments, we refer to the data published by Kaufman et al. (2020).

2.2. Transient model simulations

The model data from the nine different models are shown in Table 2 with the experimental setup for each simulation. Because the simulations are transient, they start from boundary conditions of the past climate (exact starting time varies) and then simulate the climate up through the Holocene, based on timevaried values of different forcings. The simulations are not done specifically for this

Table 1
Climate variables represented in the proxy records.

Terrestrial (number of records)		Maritime (number of records)	
Air temperature	67	SST	36
Lake surface temperature	3	Sea ice	3
Effective moisture	10		
Precipitation	1		

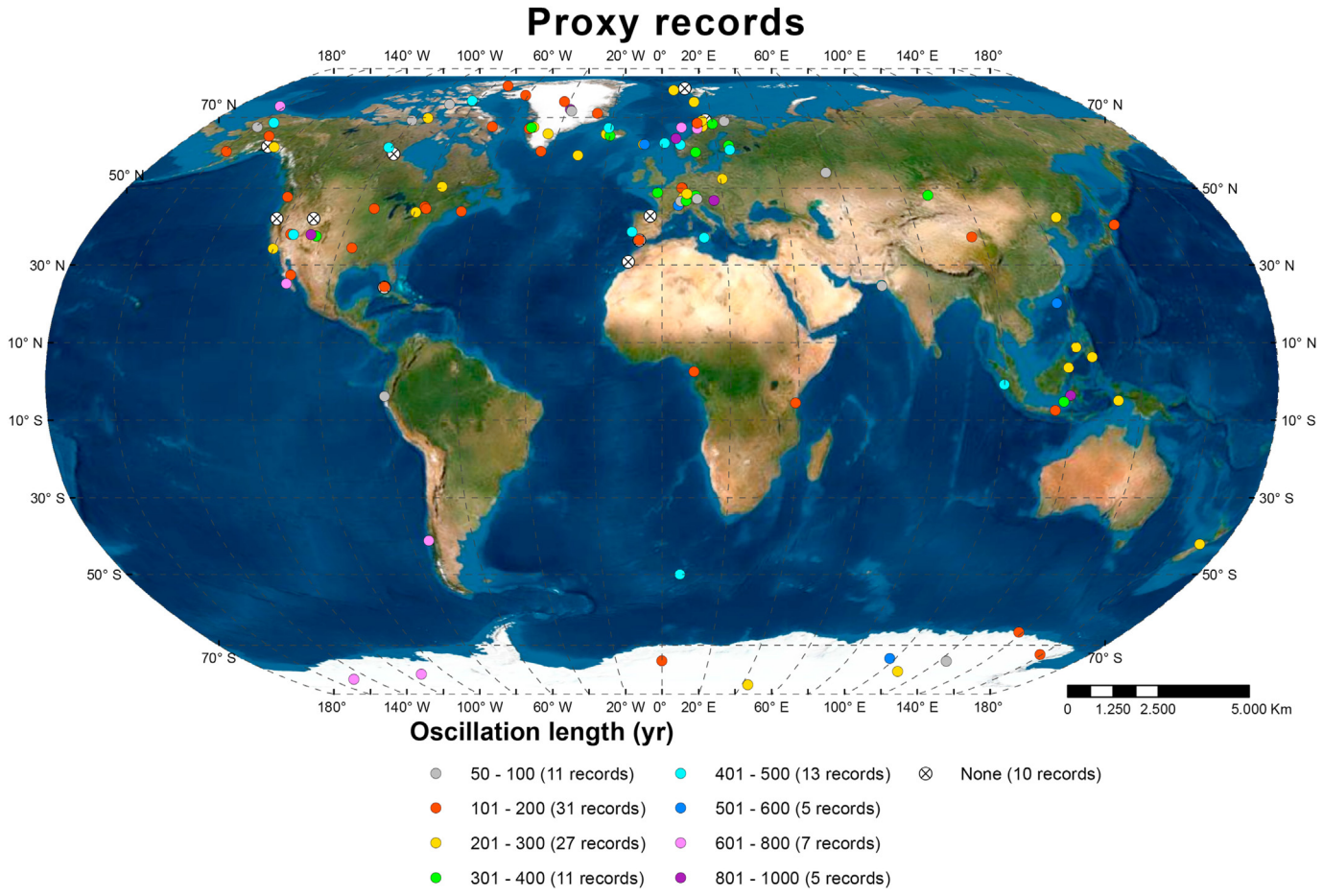

Fig. 1. Location of the proxy records with symbols colorized based on the period length of the highest density peak. Base-map derived from Esri (2022).

collaborative work, so as Table 2 shows, some differences exist in the transient forcings included in the different models, so a complete forcing scenario or *full forcing* for each model is not the same across the ensemble. Time varied solar irradiance is, for example, only included in CESM1, HadCM3, MPI-ESM, and NNU 12k, while the rest use a fixed value.

Temperature is the only variable analyzed from the model data, so the temperature proxies are the most relevant group for the model-proxy comparison. Proxies mainly reflect temperature conditions near the surface, so we attempt to make the model data more comparable by using surface temperature (*ts*) for AWI-ESM, CESM1, LOVECLIM, NNU12k, and TraCE. We use the 2 m near surface air temperature (*tas*) for the other models. As we focus on climate variability, this is not expected to impact the results in the frequency domain.

All simulations cover at least 5900 years, with CESM1 being the shortest with 5900 years, and HadCM3, LOVECLIM1.3, NNU 12k and TraCE cover at least 10.000 years. NNU 12k and TraCE extend back to 12,000- and 22,000-years BP, respectively, but only the Holocene part is used for the spectral analysis. AWI-ESM consists of two separate simulations with a 500-year overlap, and we treat them as two different outputs throughout the analysis. The annual mean data from the model output is analyzed for global mean temperature (GMT) and six latitude bands (90°N–60°N, 60°N–30°N, 30°N–0°, 30°S–0°, 60°S–30°S, and 90°S–60°S) to test for any potential dependencies on latitude.

HadCM3, LOVECLIM, MPI-ESM, NNU 12K, and TraCE are the five models with additional differentiated forcing simulations with a total of 14 extra simulations, and for these, we only consider GMT. As these are not explicitly created to be compared within this work, they have some differences in the simulation setup. TraCE uses a single forcing approach while the others have differentiated forcing setups in the individual simulations. We show the details about which forcings are included in the different simulations in Table 3. Since the TraCE simulations originally were more extended, the single forcing scenarios fix the other forcings at conditions from around 20.000 BP (exact time varies for different forcings). Hence, the TraCE single forcing simulations might not be as representative

Table 2
Details of the models used. * Only data from 10.000 to 0 BP is used in the analysis. BP is relative to 1950.

	AWI-ESM2	CESM1	EC-Earth-veg-LR	HadCM3-M2.1d	IPSL	LOVECLIM1.3	MPI-ESM1.2	NNU 12k	TraCE
Atmospheric module	ECHAM6	CAM5	IFS 36r4	HadAM3	LMDZ	ECBilt	ECHAM6	CAM5	CAM3
Atmospheric grid	1,875° x 1,875°	3,75° x 3,75°	1,125° x 1,125°	3,75° x 2,5°	2.5° x 1.27°	5,61° x 5,61°	1,875° x 1,875°	3,75° x 3,75°	3,75° x 3,75°
Atmosphere Vertical	47 levels	26 levels	62 levels	19 levels	39 levels	3 levels	47 levels	26 levels	26 levels
Ocean module	FESOM2	POP2	NEMO3.6	Gordon et al. (2000)	NEMO3.6	CLIO	MPI-OM	POP2	POP
Ocean grid	1°	3°	1°	1,25° x 1,25°	2°	3° x 3°	1,5°	3°	3,6°
Ocean vertical	48 levels	60 levels	75 levels	20 levels	31 levels	20 levels	40 levels	60 levels	25 levels
Sea ice module	FESOM	CICE4	LIM3	Gordon et al. (2000)	LIM2	CLIO	MPI-OM	CICE4	CSIM
Ice sheets	PISM	Glimmer CISM	No	ICE-6G	No	CLIMBER-2	No	No	ICE-5G
Vegetation	Dynamic	Dynamic	Dynamic	Dynamic	Dynamic	Dynamic (reduced form)	Dynamic	Dynamic	Dynamic
Land-surface module	JSBACH	CLM4	HTESSEL	MOSES 2.1	ORCHIDEE	VECODE	JSBACH	CLM4	CLM3
Orbital forcing	Berger (1978)	Berger (1978)	Berger (1978)	Berger (1978)	Berger (1978)	Berger and Loutre (1991)	Berger (1978)	Berger (1978)	Berger (1978)
Green house gases	Köhler et al. (2017)	Flückiger et al. (2002)	Köhler et al. (2017)	Veres et al. (2013)	Köhler et al. (2017)	Lüthi et al. (2008)	Brovkin et al. (2019)	Joos and Spahni (2008)	Joos and Spahni (2008)
Solar irradiance	No	Vieira et al. (2011)	No	Vieira et al. (2011)	No	No	Krivova et al. (2011)	Vieira et al. (2011)	No
Land use forcing	No	No	No	HYDE 3.2 + KK 10	No	No	Hurtt et al. (2011)	HYDE 3.2	No
Volcanic eruptions	No	No	No	Sigl et al. (2022)	No	No	Zielinski et al. (1996)	No	No
Time (years BP)	9000–0	6000–100	8000–0	10000–0	6000–0	10000–0	7949–0	12.000–0*	21.000–0*
Citation	Shi et al. (2020, 2021)	CESM Software Engineering Group CSEG (2020)	Zhang et al. (2021)	Hopcroft and Valdes (2022) Hopcroft and Valdes (2021)	Braconnot et al. (2019)	Yin et al. (2021)	Dallmeyer et al. (2020) Bader et al. (2020) Mauritsen et al. (2019)	Sun et al. (2020)	NCAR (2011)
Institution	AWI	Fudan Uni.	Stockholm Uni.	Uni. Of Birmingham	LSCE/IPSL	Uni. catholique de Louvain	MPI	Nanjing Normal Uni.	NCAR

Table 3
Forcings included in the differentiated forcing simulations.

Forcing							
	Orbital	Solar irradiance	GHG	Volcanic	Land use	Ice sheet	Melt water flux
HadCM3 OrbGHGICE	x		x			x	
HadCM3 +Sol	x	x	x			x	
HadCM3 +SolVolc	x	x	x	x		x	
HadCM3 +SolVolcHYDE	x	x	x	x	HYDE 3.2	x	
HadCM3 +SolVolcKK10	x	x	x	x	KK10	x	
MPI-ESM all	x	x	x	x	x		
MPI-ESM OrbGHG	x		x				
LOVECLIM Orb	x						
LOVECLIM OrbGHG	x		x				
LOVEVLIM OrbGHGICE	x		x			x	
NNU 12k ORBIT	x						
NNU 12k TSI2	x	x					
NNU 12k LUCC	x				x		
NNU 12k GHG	x		x				
TraCE ORB	x						
TraCE CO2			x				
TraCE MWF							x
TraCE ICE						x	
Trace all	x		x			x	x

of the Holocene as the other three models, e.g., large NH ice sheets are still present. NNU 12k does not have a simulation with all its forcings included, so the *GHG* simulation is chosen to represent this model alongside the full forcing simulations from the other models. For HadCM3, the *+SolVolcKK10* experiment is used as the full forcing scenario, and the *+SolVolcHYDE* includes the same forcings but with a different source for anthropogenic land use. MPI-ESM has a simple scenario, *OrbGHG*, with only orbital and greenhouse gas forcing and a full scenario (labelled *all*) which also includes solar irradiance, volcanic eruptions, and anthropogenic land use, although land use is only partially included in the last 1000 years (850-1849 CE) of the simulation.

2.3. Spectral analysis

As multi-centennial variability is the focus of this work, we have removed the high-frequency noise using a low-pass Butterworth filter in both the proxies and model data. As the Butterworth filter works on regularly spaced time series, the proxy data are interpolated with an Akima interpolation (Akima, 1970) to a 10 year, evenly spaced resolution as some of the original records have irregular sampling intervals. As the orininal resolution of the proxy records spans from 1 to 50 year, some records are downsampled by the resolution while others are upsampled by the interpolation. After the interpolation, the butterworth filter is used to filter out oscillations with frequencies higher than 20 years. This procedure is applied to all the records, regardless of the archive or proxy type to provide a uniform handling of the records in the pre-processing stage and effectively mainly filter the records where it is necessary (where the original resolution is better than 20 years). The procedure does open up for potential interpolation biases, but the alternative of using different approaches to different proxy types would not be free of uncertainties either and when the aim of this study is to compare a large and diverse proxy group (archive and proxy type, location, record length, etc.) the uniform approach is chosen.

The model data generally contains more high-frequency variability than the proxies due to the better temporal resolution and because some proxies naturally filter climate signals (Evans et al., 2013; Dee et al., 2015). Therefore, we set the filtering value to 60 years instead of 20 years for the model data, which is found to be more suitable even though multi-centennial variability can still be seen with the 20-year filter, as too much spectral density is distributed over the multi-decadal range, potentially clouding some of the slower multi-centennial oscillations. The upper part of the multi-decadal range is still preserved with the 60-year filter and the detail in the multi-centennial range is better. Therefore the 60-year filter is chosen for the analysis of the model data.

The spectral analysis is done with the program 'REDFIT' developed by Mudelsee (2002) in a version adapted to the R package by Bunn et al. (2021), which also includes a significance test against red noise at the 95% significance level. A large amount of data generate many spectra, and we therefore apply kernel density distributions to help illustrate the results in the different proxy and model groups. The kernel density distribution is calculated with a Fourier transform and linear approximation to estimate the density at different points (Sheather and Jones, 1991) and thereby how the significant periods are distributed over the centennial range.

3. Results

3.1. Multi-centennial variability in proxy records

The spectral analysis of the proxy data reveals significant variability cycles in most records. Only 10 out of the 120 records contain no significant spectral peaks. Fig. 1 shows the location of the proxy records and a colour grouping based on the period of the significant oscillation. Only the peak with the highest spectral density is included on the map. Fig. 1 shows no apparent distinction in the oscillation period based on the geographical location (on a global scale at least). The same can be said of the 10 records with no significant oscillations. The different oscillations are not confined to specific regions, and we find the shortest (50–100 years) and longest groups (601–1000 years) in both the Northern and Southern hemispheres. The same is true for the 10 records that did not show any significant oscillations. Fig. 1 also shows the number of records in the different groups of the oscillation period. The two groups between 101 and 300 are the largest, with 31 and 27 records between 101-200 and 201–300, respectively. We provide the details of the individual records and their periods in Table 2.

As many records have more than one significant spectral peak, Fig. 2 shows the distribution of the oscillation periods found in the proxies, and includes up to three significant peaks per record. Considering all proxies in one group (Fig. 2a), the most common oscillation period at multi-centennial timescales is between 100 and 250 years, and the average is 240 years. There are also many records in the upper part of the multi-decadal range (50–100 years), but the number of significant oscillations longer than 300 years is few in comparison.

The two big groups of climate variables, temperature and SST (Fig. 2b and c), generally show the same distribution when considering them individually. However, SST is slightly flatter and less concentrated around the 100–250 years period. The other climate variables are too few to make any conclusions on their distribution, but they are not confined to any specific part of the multi-centennial range.

As the temperature records are the most extensive group, they are also made from the highest number of different archives, so they can be further sub-grouped based on the archive type, as shown in Fig. 2d. The grouping indicates that the different kinds of archives contain the multi-centennial oscillation signal, so there is no indication that the few outlying long oscillations are caused by a specific archive type, as the four longest oscillations found are from four different types (speleothems, midden, ice core and peat).

As mentioned earlier, there is a bias toward NH mid-to-high-latitudes. Despite this, the lack of dependencies on region, climate variable and archive type for the oscillation period indicates that multi-centennial variability has indeed been a large-scale feature of the Holocene climate, according to the proxy evidence.

3.2. Multi-centennial variability in transient model simulations

The evolution of the global mean temperature in transient simulations is shown in Fig. 3. There is a large spread between the models of almost 5 °C at 10.000 BP and 4 °C at present. To this point, it should be noted that some are surface temperature (*ts*) while others are near surface air temperature (*tas*), but neither of the two groups is consistently warmer or colder. The amplitude of variability in the different time series also varies between the models, with EC-Earth showing the highest amplitude up to ~ 0.5 °C and down to ~ 0.1 °C in LOVECLIM and CESM1. So, despite all being transient simulations, there are some apparent distinctions between the models, which could be related to different forcings in the simulations, and overall model performance, including model resolution.

The spectra from the full forcing simulation GMT (Fig. 4) show that all models exhibit significant spectral power in the multi-centennial range, with most at frequencies corresponding to periods of 100–200 years. There are some longer oscillations up to 400 years in HadCM3 and CESM1, while AWI-ESM has the peak with the highest spectral density below 100 years. The other models have the highest spectral peak in the 100–200-year range. We also observe significant multi-decadal peaks, indicating the filter does not dampen the oscillations too much. The exact timing of the spectral peaks varies between the models alongside the spectral density. There are differences in the variability signals they produce, as indicated by their time series in Fig. 3. The overall results show a good agreement among the models regarding the presence of significant oscillations of 100–200 years in the GMT.

The spectra for the different latitude bands show significant peaks at frequencies corresponding to 100–200 years (Fig. 5), indicating the multi-centennial variability has no obvious dependencies on latitude. Comparing the latitude bands within each

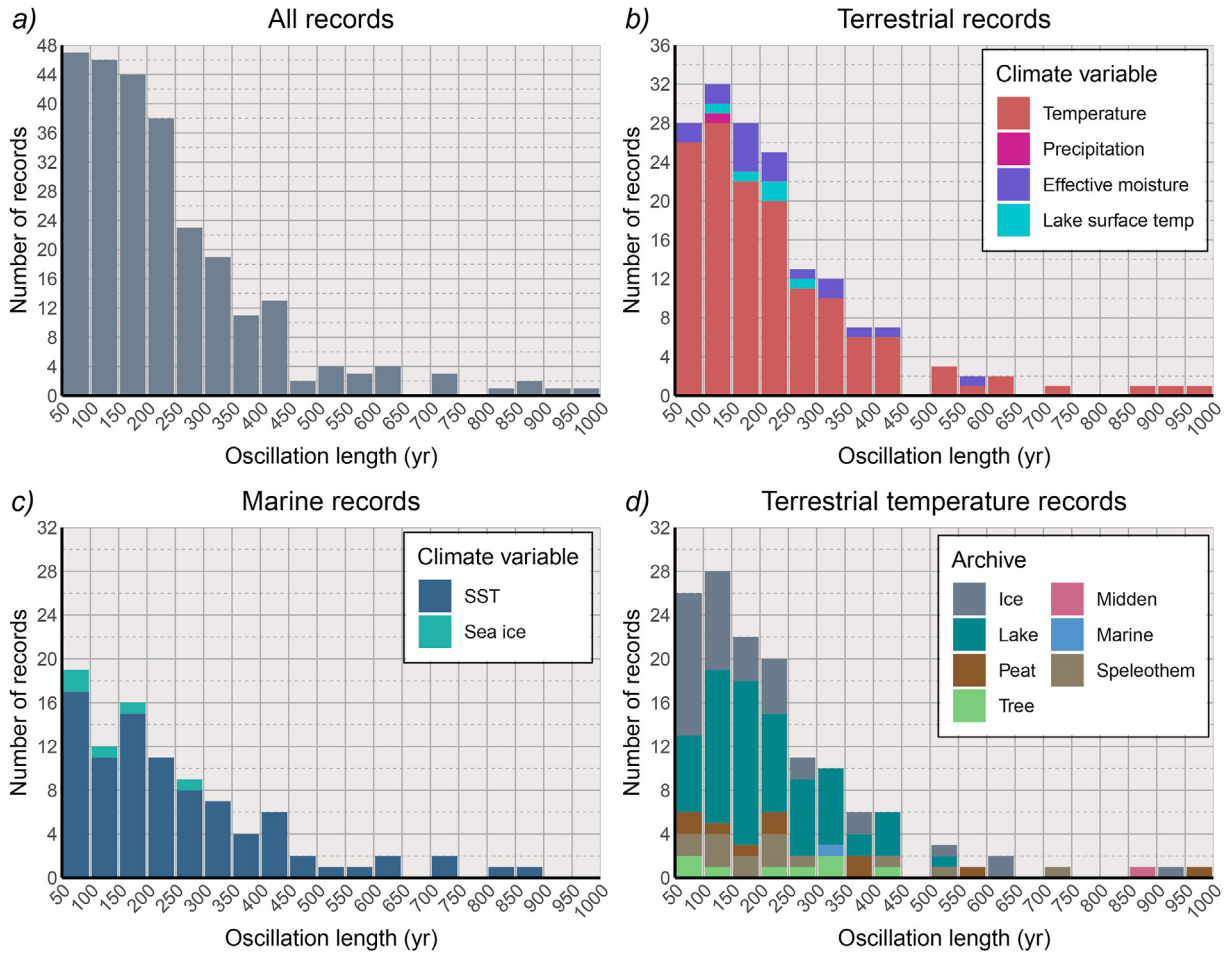

Fig. 2. Length of the significant oscillations found in the proxy data. Up to three spectral peaks are included per record. All records are included on a, b and c are separated into climate variables, and d is air temperature separated into archive type.

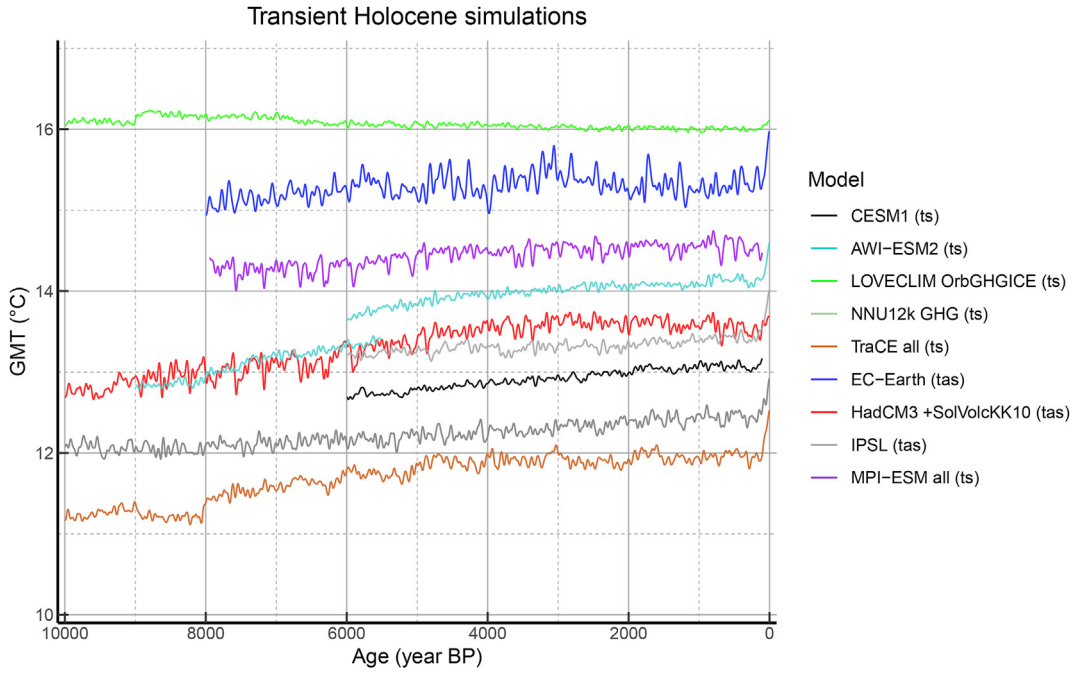

Fig. 3. Global Mean Temperature time series of the full forcing transient Holocene simulations filtered with a 60-year low-pass Butterworth filter. Age before present (BP) is relative to 1950.

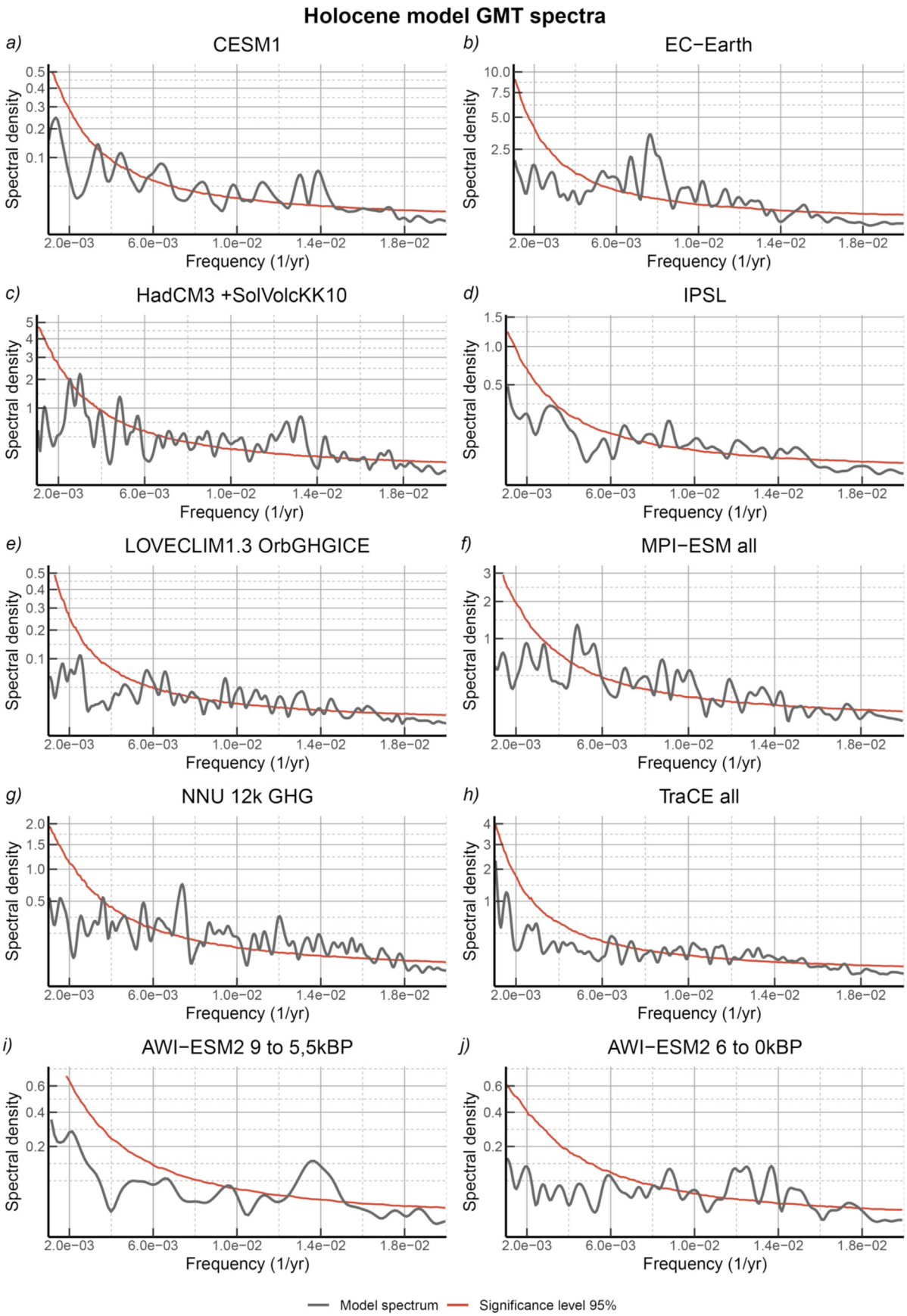

Fig. 4. Spectra of model GMT from transient Holocene simulations filtered with a 60-year low-pass Butterworth filter. The red Lines show the 95% significance level from red noise. (For interpretation of the references to colour in this figure legend, the reader is referred to the Web version of this article.)

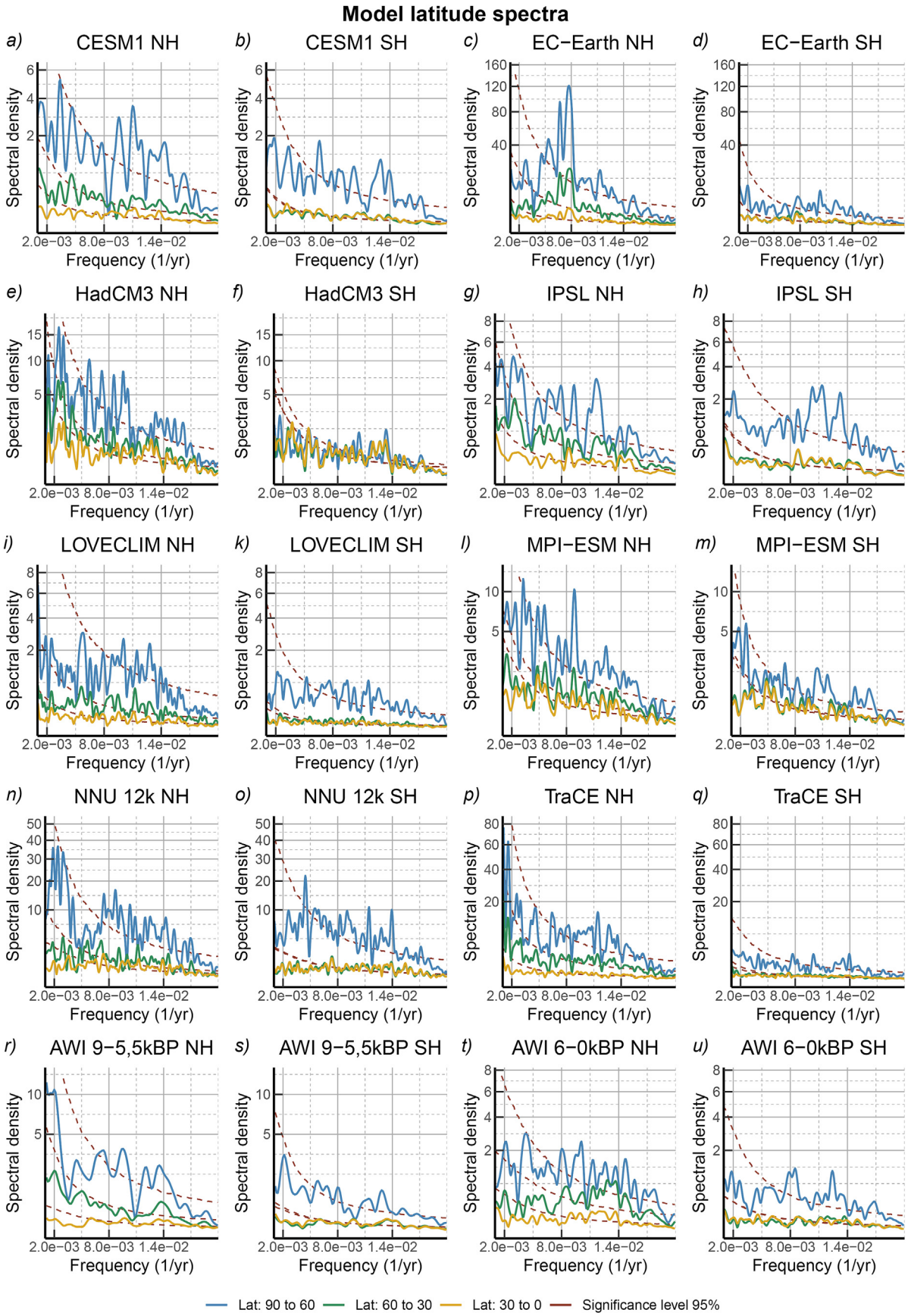

Fig. 5. Spectra from transient Holocene model simulations in different latitude bands, separated into Northern and Southern hemisphere for each model.

model to each other, we noted the following four points: 1) most spectral density is distributed over the 90°N–60°N band, which could indicate extra sensitivities to the variability or potential driving mechanisms arising from the region. 2) The 60°N–30°N and 30°N–0° bands generally follow the same trajectory as the 90°N–60°N band, with the 60°N–30°N band always being situated higher in spectral density. 3) The 60°S–30°S and 30°S–0° bands are very similar in both trajectory and spectral density for all models, and therefore have the same variability signals, which could indicate that the drivers and feedbacks affect these two bands in a similar fashion. 4) The 90°S–60°S band contain subtly different spectra from the other bands in several models. However, in some such as EC-Earth and HadCM3, it still follows the same general trajectories, so there are discrepancies between how the models reproduce the Antarctic variability. This is also the case when looking at the spectral density relative to the Northern hemisphere bands, where it can be either higher or lower than the 60°N–30°N band, depending on the model. However, it consistently has the highest spectral density in the SH, which could potentially be induced by the bipolar seesaw modulated by AMOC strength, if the variability is NH driven.

The models support the proxies regarding the absence of any notable latitude dependency upon having significant oscillations at multi-centennial timescales. There is an indication of the Arctic being a region of interest for feedback mechanisms or potential drivers as more spectral density is distributed over this latitude band. Further investigation of multi-centennial variability in this region is a highly relevant topic. To this point, it should also be noted that the cryospheric feedbacks in the Arctic could be a potential source of this increased variability, so these results might not be surprising.

The spectra from the differentiated forcing simulations in Fig. 6 all show significant peaks at frequencies corresponding to a 100–200-year period. This is also the case in the most basic transient setup using only orbital forcing. The other forcings all induce some variability to the system and, in some cases, alter the exact oscillation period or the trajectory of the spectra, but the multi-centennial variability is always present. Anthropogenic land use seems to have a lesser impact than the other forcings, which could be due to minor change before ~4000 BC. Solar irradiance and volcanic eruptions alter the spectra, impacting the variability signals produced as they contribute to multi-decadal variability. In HadCM3, the volcanic eruptions clearly have a larger impact on multi-decadal variability than solar irradiance, so this appears to be an important forcing for the variability in this frequency range, which is also supported by Mann et al. (2021). However, the results do not support any of them being the main driver on multi-centennial timescales. For example, not all the models include solar irradiance, but they still produce significant multi-centennial variability.

3.3. Proxy-model comparison

To see how the variability in the proxies compares to the model results, we plot the kernel density distribution of the proxies with those from the model latitude bands and GMT in Fig. 7 (differentiated/single forcing simulations not included). We created two kernel density distributions from the proxies, with the dark red being all proxy records and the pink being only those representing temperature, as it is the most comparable to the model results. However, Fig. 7 shows barely any difference between these two, even though the pink distribution only includes temperature and the dark red have all the climate variables from the proxy ensemble, implying that this distinction is not important.

The kernel density distributions from the proxies peak at ~120 years, so they are situated very close to those from the model data, which peak around 100 years on average. The average period for the proxies is ~240 years, and hence clearly longer than those from the models, which have an average period of around 130–160 years. In the analysis of the proxies, we also find significant oscillations with periods of up to 1000 years, so this will naturally make the average higher compared to the models, where only one oscillation longer than 400 years is found (a 410-year oscillation for 60°N–30°N in HadCM3).

The kernel density distributions from the proxies are flatter than those from the models, but this is logical when considering the more diverse origin of the proxy records. Even though the climate models have their differences in both the model cores and the forcings included in these simulations, they still share the same principles that render them more homogeneous. The same cannot be said for the heterogeneous collection of proxies, where the natural processes that capture the climatic signal, the way they are reconstructed, the climatic variable they represent, and their temporal resolution all differ in the analyzed records. Some discrepancies therefore exist between the proxy and model data, as the two distributions in Fig. 7 still have their differences, so it is still possible that some modes of natural variability are not produced by the models even with solar irradiance and volcanic forcing. Combining the oscillations from the models into individual kernel density distributions (three oscillations from each latitude band and GMT) in Fig. 8 shows that HadCM3 is the model which distribution matches best with the proxies, as this is the model that most consistently produces longer periods in the different latitude bands. The distribution from MPI-ESM is also oriented more towards longer periods and is the second closest to the proxies in mean value after HadCM3. As these two models also have the complete forcing scenarios (see Table 2), with volcanic eruptions, solar irradiance, and land use, it indicates that these external forcings still are important to the variability signals, despite not finding clear evidence of any being the main driver in the differentiated forcing simulations.

Despite some discrepancies between the proxies and individual models, there is still a good agreement that there is significant multi-centennial temperature variability globally, with the majority of the oscillations having periods around 100–200 years and a ~100 longer average for the proxies due to the slightly flatter distribution.

4. Discussion

4.1. Proxy records

Most of the proxy records and all the model data examined with spectral analysis show significant variability on multi-centennial timescales, despite having different origins and characteristics. The proxies show more variety in terms of period lengths with a more spread-out kernel density distribution in Fig. 7 and longer periods than in the model data. The proxy records represent a more diverse data group with the different proxy types and reconstructions methods used to produce the records, which may alter how variability is captured. Although this is logical reasoning, it is not an inevitable fact, as no clear distinction is found between the different groupings used in the analysis. Also the precipitation and moisture records only come from the Arctic compilation of Sundqvist et al. (2014), we cannot attest to the universal nature of multi-centennial variability in all climate variables. For example, it may be the case that monsoon rainfall shows no multi-centennial variability and that the Arctic variability only occurs due to the

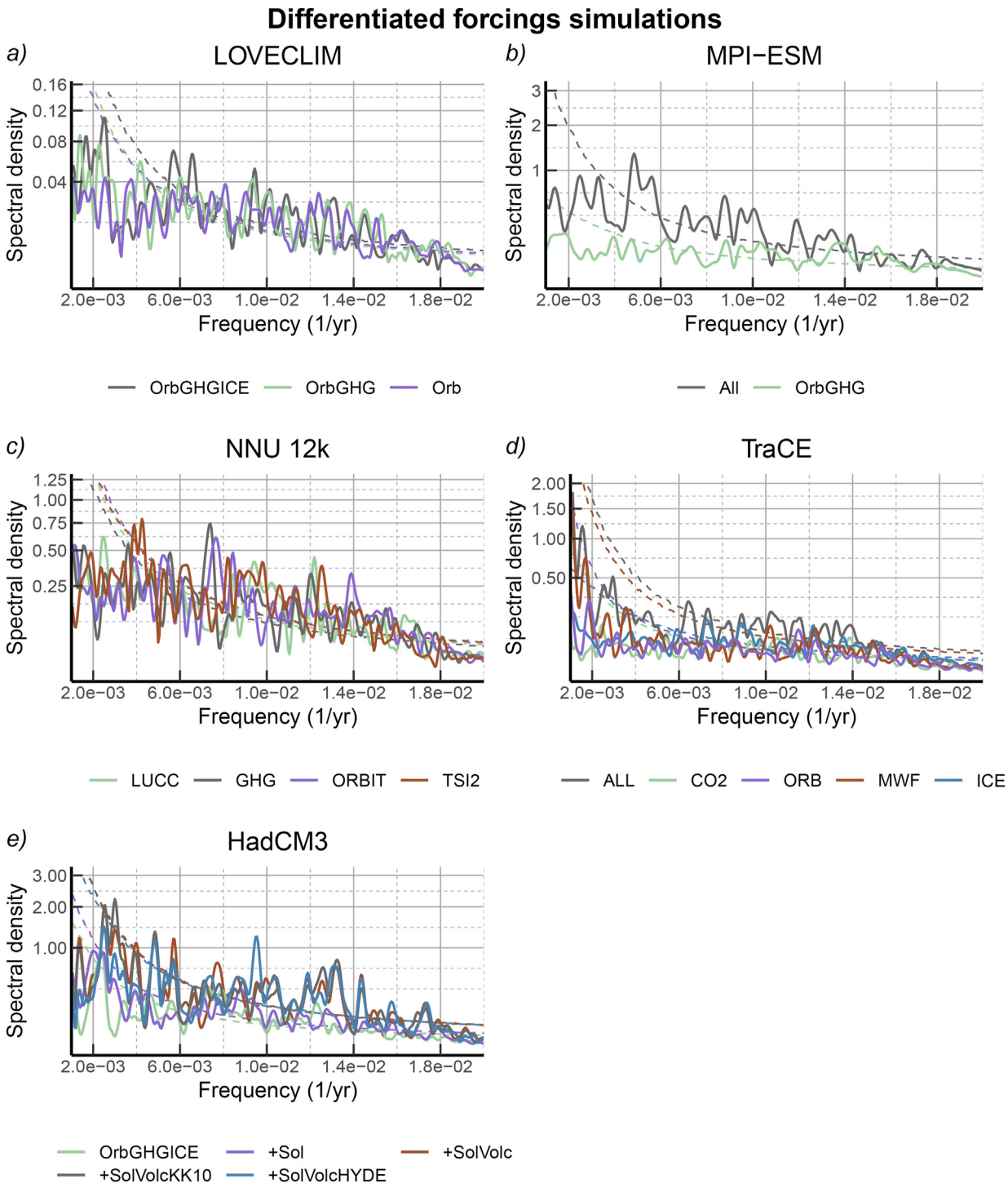

Fig. 6. Spectra of GMT from differentiated forcing simulations. The dash line marks the 95% significance level relative to a red noise spectrum. The included forcings in the individual simulations can be seen in Table 3. (For interpretation of the references to colour in this figure legend, the reader is referred to the Web version of this article.)

strong temperature dependence of snowfall in the region. Further work would be needed to explore that possibility.

The generic uncertainties related to dating, local factors and seasonality bias are potential sources of error in this analysis. Age uncertainty is not assessed in this study, but the analysis relies on the quality assessment done by Sundqvist et al. (2014) and Kaufman et al. (2020). As the analysis only depends on the relative age sequence and not the absolute values and synchronicity between the records, it is not expected to be considerable uncertainty in the results. Weaknesses in the chronology would, in this analysis, mainly obscure the results by adding noise, as we only examine the existence of low frequencies and not precisely when they occur and whether they are synchronous or not. Future work needs to consider the potential temporal changes in the variability signals in more detail, and here chronological and synchronicity uncertainties will be even more important to account for.

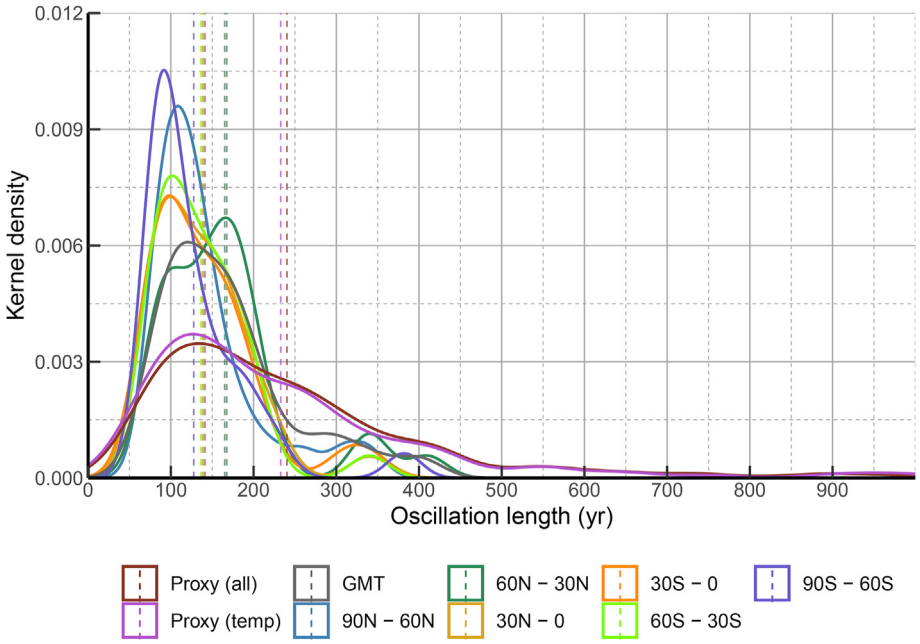

Fig. 7. Kernel density distribution of the oscillations found in the proxy and model data for the GMT and different latitude bands (up to three spectral peaks per time series). The dash line marks the mean of the group. All the groups not named proxy are from the model data.

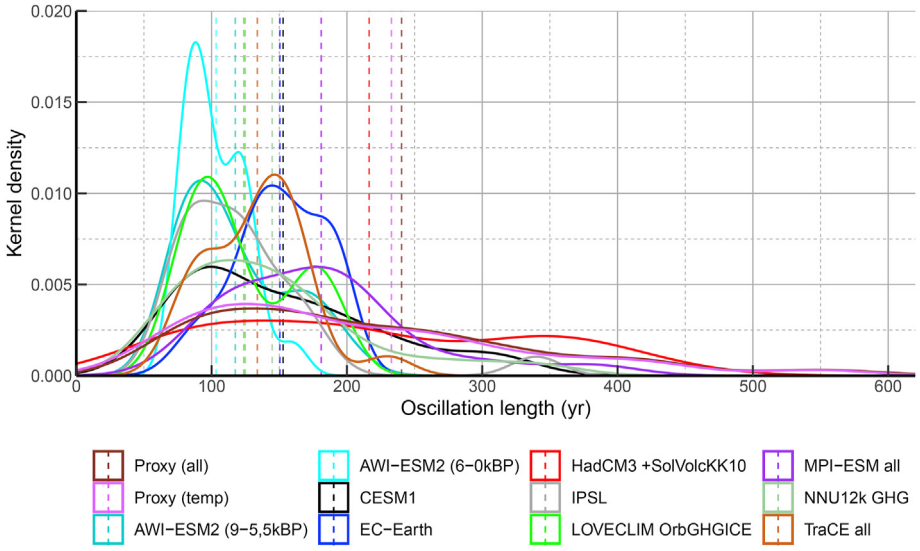

Fig. 8. Kernel density distribution of the oscillations found in the proxy and model data, where all latitudes bands and GMT are combined for each model (up to three spectral peaks per time series). The dash line marks the mean of the group. The upper part of the proxy distribution (> 600 years) is not included, see Fig. 7 instead.

Uncertainties related to local factors are mainly mitigated in this work via using a large ensemble of records and focussing on the general variability evidence. Focussing more on individual records would require the inclusion of this. The outliers with longer periods might be related to local factors at these sites.

In the original publications for the individual proxy records, multi-centennial variability is often mentioned as an apparent feature in the constructed time series, and it has only been examined with spectral analysis in a few cases. Generally, the significant peaks in the original papers are similar to the ones found in this analysis, but sometimes without complete alignment, as different methods and approaches are used for the analysis (Staubwasser et al., 2002; Sarnthein et al., 2003; Helama et al., 2010; Berner et al., 2008; Ersek et al., 2012; Yu, 2013; Kuhnert et al., 2014). Some papers on the proxy records have noted multi-centennial variability but did not quantify it with statistical analysis (Lamy et al., 2002; Andresen et al., 2004a, 2004b; Kim et al., 2004, 2007; Williams et al., 2005; Anne de Vernal et al., 2005; Weldeab et al., 2007; Ojala et al., 2008; Seppä et al., 2009; Belt et al., 2010; Berner et al., 2010; Martin-Chivelet et al., 2011; Larsen et al., 2012; Balascio and Bradley, 2012; Zhao et al., 2013; Salzer et al., 2014; Boldt et al., 2015; Shuman and Marsicek, 2016; Baker et al., 2017; Mezgec et al., 2017). Our analysis now confirms their initial qualitative observations. In addition, the periods in this analysis agree with a proxy study by Taricco et al. (2015), who finds common oscillations of 100–200 years in 26 proxy records across different latitudes.

4.2. Model evidence

The model results in this analysis agree with the proxy-based study by Taricco et al. (2015) regarding period length and a lack of latitudinal dependency in showing significant oscillations. However, the studies based on long transient model simulations to compare with are limited, as the simulations only recently have become available. Model performance over such long timescales is thereby also a relatively new issue. Some of the model differences in their time series and the spectral density could be related to this. It could be associated with the different experimental setups, because these simulations are not created to be a uniform ensemble. Organised coordination with specific protocols, such as standard setups with orbital, GHG and ice forcings and a realistic scenario with volcanic and solar irradiance included, would benefit studies like this one, as model ensembles are essential to mitigate model biases and uncertainties.

The TraCE simulations have been available for the longest time. The simulations have been used in a study by Zhu et al. (2019), which is the only study with spectral analysis of a transient simulation longer than the past millennium with a GCM. The study by Zhu et al. (2019) used the entire length of the TraCE simulation and the spectral peak they identified at 170–180 years is close to 160 years in our analysis (for GMT). Variability at multi-centennial timescales is also observed (without spectral analysis) in Braconnot et al. (2019) and Bader et al. (2020), and this analysis then confirms its presence.

4.3. Potential drivers

Finding the drivers of variability can be difficult, as it is hard to distinguish between forced variations projected on natural mechanisms and internal variability (Laepple and Huybers, 2014a). The different forcings in the differentiated forcing simulations do alter the distribution of spectral density slightly (some forcings more than others) in the individual models. However, no major differences are observed in having significant oscillations at multi-centennial timescales. Instead, the exact period lengths change with the differentiated forcing simulations. This is also the case with the simulations that only include the slow orbital forcing, although the amount of spectral density is often situated slightly lower. The spectral analysis of the differentiated forcing simulations implies that the different forcings induce some variability to the climate system. Still, none is the primary driver of the multi-centennial variability, as it is always present.

Internally driven centennial variability is in contrast to some papers from proxy reconstructions, including some used for this analysis that suggests solar irradiance be the primary driver (e.g. Sarnthein et al. (2003); McKay and Kaufman (2014); Salzer et al. (2014)). The hypothesis of solar-driven variability often stems from period alignments between climate reconstructions and solar irradiance. The Suess/De Vries solar cycle, which oscillates with 190–210 years Stefani et al. (2021), is also in good alignment with the periods found in this analysis, and it is a well-accepted feature of the sun's behaviour from both proxy studies (Beer et al., 1994; Beer, 2000; Bond et al., 2001; Ogurtsov et al., 2002; Stefani et al., 2021) and modelling of the solar system dynamics (Wilson, 2013), so it is still possible that it impacts the variability signals (Sun et al., 2022).

Solar irradiance is, however, not the only proposed driver as other internal mechanisms, such as the AMOC (Stuiver et al., 1995; McDermott et al., 2001; Rimbu et al., 2004; Wirtz et al., 2010) and Arctic sea ice (Müller et al., 2012; Hörner et al., 2017; Lapointe et al., 2020) is suggested as potential drivers or at least related feedbacks in other proxy studies. The higher amount of spectral density in the NH high latitudes found in this analysis indicates the high relevance of driving mechanisms and/or feedbacks concentrated in this region. It is plausible that some internal mechanisms operate on multi-centennial timescales. Several climate modelling studies using long control simulations attribute the source of multi-centennial variability to fluctuations of AMOC (Vellinga and Wu, 2004; Park and Latif, 2008; Friedrich et al., 2010; Delworth and Zeng, 2012; Jiang et al., 2021). Vellinga and Wu (2004) pointed out that AMOC drives the northward shift of the intertropical convergence zone (ITCZ), leading to the tropical salinity anomaly and propagating to the subpolar North Atlantic. Park and Latif (2008) and Delworth and Zeng (2012) emphasized the importance of freshwater anomalies from the South Atlantic transporting northward alongside AMOC. Some studies argue that salinity anomalies come from the Arctic Ocean dominated by freshwater exchanges between the Arctic and North Atlantic regions (Hawkins and Sutton, 2007; Yin et al., 2021). Recently, using simple conceptual models, Li and Yang (2022) identified theoretically a self-sustained multi-centennial mode in the AMOC by introducing an enhanced mixing mechanism in the subpolar ocean.

The multi-centennial variability may consist of external forcing and internal mechanisms. If the timing and period lengths do not always align, it will leave a complex signal when the contributors go in and out of phase with each other. If that is the case, the variability signal would be irregular through time. Analyzing the temporal dependency of the variability would help uncover this further, as that has not been a part of this analysis and some proxy time series are characterized by a change of frequency during the late Holocene (Allan et al., 2018; Bae and Chatzidakis, 2022).

5. Conclusions

This study has first attempted to analyze coherent variability signals at multi-centennial timescales in transient Holocene model simulations from GCMs and a compilation of 120 proxy records. This was done with the aim of finding the overall conclusions related to period length and potential latitudinal dependencies, as well as discussing the potential drivers through differentiated forcing simulations.

Broad scale multi-centennial variability with significant oscillation periods of 100–200 years is evident across both the model simulations and proxy data, and we found that it is a global signal. There is, however, more spectral density distributed across the NH high latitudes, which could be related to extra sensitivity or potential driving mechanisms concentrated in the region.

None of the external forcings is found to be the sole driver of the variability, which further highlights the importance of future studies of the Arctic to find potential internal drivers and/or essential feedbacks. As the external forcings still induce some variability to the system and variations in solar irradiance are a well-documented feature of the sun at multi-centennial timescales, a set of drivers may have impacted the multi-centennial variability in the Holocene. Volcanic forcing does also contribute to the variability and increases the spectral density, when included in the model, so further research is needed to examine potential drivers more closely and thoroughly. In addition, both the model and proxy data vary in their age coverage despite all being located in the Holocene and the proxies are not synchronized, so further research into any potential changes in the variability pattern through time with, e.g., wavelet analysis, is a relevant aspect of both future research into potential drivers and testing/elaborating on the results of the analysis of this paper.

Author contributions

Thomas Gravgaard Askjær: Conceptualisation, Methodology, Data curation, Formal analysis, Investigation, Visualisation, Writing – original draft, Revision. **Qiong Zhang**: Conceptualisation, Data curation, Review & Editing, Project administration, Funding acquisition, Supervision. **Frederik Schenk**: Methodology, Review & Editing. **Fredrik Charpentier Ljungqvist**: Review & Editing. All the other coauthors provide the model data and commented the manuscript.

Declaration of competing interest

The authors declare that they have no known competing financial interests or personal relationships that could have appeared to influence the work reported in this paper.

Data availability

Climate model simulation data will be made available on request.

Acknowledgements

This work was supported by the Swedish Research Council (Vetenskapsrådet, Grant No 2017-04232). Frederik Schenk is funded by the Swedish Research Council for Sustainable Development (FORMAS 2020-01000). F.C.L. was supported by the Swedish Research Council (Vetenskapsrådet, Grant No 2018-01272), and conducted the work with this article as a Pro Futura Scientia XIII Fellow funded by the Swedish Collegium for Advanced Study through Riksbankens Jubileumsfond. Haijun Yang is funded by NSF of China (No. 42230403). The EC-Earth Holocene transient simulations and the data analysis were performed using ECMWF's computing and archive facilities and the Swedish National Infrastructure for Computing (SNIC) at the National Supercomputer Centre (NSC) partially funded by the Swedish Research Council through grant agreement no. 2018–05973. Computational resources for the LOVECLIM1.3 transient simulations have been provided by the supercomputing facilities of the Université catholique de Louvain (CISM/UCL) and the Consortium des Équipements de Calcul Intensif en Fédération Wallonie Bruxelles (CÉCI) funded by the Fond de la Recherche Scientifique de Belgique (F.R.S.-FNRS) under convention 2.5020.11. We acknowledge constructive comments from Anders Moberg on terminology in describing the variability.

Appendix

Table 4
Details on the proxy records from Sundqvist et al. (2014) and Kaufman et al. (2020) used for spectral analysis and their significant periods displayed in the order of the highest spectral density (only the three highest density cycles). Effective moisture is shortened to moisture and LST is lake surface temperature. If comments are made in the quality control by Kaufman et al. (2020), it is marked "y" in the "QC com" column.

Record	Lat (°)	Lon (°)	Elev (m)	Archive	Proxy	Max age	Min age)	dt (yr)	Variable	Seasonality	Citation	Period length (yr)			QC com
893A	34	−120	−588	Marine	$d^{18}O$	10002	9	30	SST	Annual	Kennett et al. (2007)	230	190	100	y
Agassiz	81	−73	1730	Ice	$d^{18}O$.ice	11640	0	20	Air temp	Annual	Vinther et al. (2009)	170	140	80	
Alsopahok	47	17	126	Peat	pollen	10679	95	36	Air temp	Annual	Zatykó et al. (2007)	1000			
Ammersee	48	11	533	Lake	$d^{18}O$	15588	−12	11	Air temp	Annual	Czymzik et al. (2013)	350	260	190	y
AMP112	80	11	35	Lake	alkenones	12353	1145	48	LST	Summer	van der Bilt et al. (2018)	None			y
Arapisto	61	25	133	Lake	pollen	8889	0	18	Air temp	Annual	Korjonen and Seppä (2007)	420	320	250	
ARC-3	74	−91	−347	Marine	IP25	10021	439	16	Sea ice	Spring	Vare et al. (2009)	80			
ARC-4	69	−101	−61	Marine	IP25	7731	83	17	Sea ice	Spring	Belt et al. (2010)	70	120		
Beef Pasture	37	−108	3060	Lake	pollen	6025	0	33	Air temp	Winter	Petersen (1985)	340			y
BJ8_03_13GGC	−7	115	−594	Marine	Mg/Ca	10593	179	42	SST	Annual	Linsley et al. (2010)	190	150	100	
Bledowo Lake	53	21	78	Lake	pollen	10996	156	41	Air temp	Annual	Binka et al. (1988)	240	170		
Braya Sø	67	−51	170	Lake	alkenones	6119	−55	44	LST	Summer	William D'Andrea et al. (2011)	290	22		y
Camp Century	77	−61	1890	Ice	$d^{18}O$.ice	11650	−10	20	Air temp	Annual	Vinther et al. (2009)	140	90		y
Cape Ghir	31	−10	−900	Marine	alkenones	10502	−28	29	SST	Annual	Kim et al. (2007)	None			y
D13882	39	−9	−88	Marine	alkenones	13106	442	22	SST	Annual	Rodrigues et al. (2010)	410	530	160	
Devon Ice Cap	75	−83		Ice	$d^{18}O$.ice	20539	39	50	Air temp	Annual	Fisher et al. (1983)	250	210	160	
Devon Island Glacier	75	−83	1800	Lake	pollen	8689	−23	42	Air temp	Summer	McAndrews (1984)	450	340	160	
Dune Lake	64	−150	134	Lake	$d^{13}C$.bulk	11326	−43	31	moisture	Annual	Finney et al. (2012)	190	110		
DurvilleTrough	−66	139	−746	Marine	diatom	10843	1000	20	SST	Summer	Crosta et al. (2007)	120	150	90	
Dye-3	65	−44		Ice	$d^{18}O$.ice	11640	−20	20	Air temp	Annual	Vinther et al. (2006)	280	70		
EDML	−75	0	2892	Ice	deterium excess	12992	1193	9	Air temp	Annual	Stenni et al. (2010)	120	170		y
Eleanor Lake	48	−124	710	Lake	BSi	10877	−49	19	Air temp	Summer	Gavin et al. (2011)	170			
Ennadai-2	61	−101	325	Lake	pollen	5392	636	31	Air temp	Winter	Nichols (1975)	420	320	250	
EPICA Dome C	−75	123	3233	Ice	deterium excess	12978	38	19	Air temp	Annual	Stenni et al. (2010)	90	110		y
Fauske	67	16	160	Speleothem	$d^{18}O$	7515	−47	26	Air temp	Annual	Linge et al. (2009)	250	160	110	
Ferndale	34	−96	263	Lake	pollen	7362	0	50	Air temp	Winter	Marsicek et al. (2018)	160			
Fiskebølvatnet	68	15	23	Lake	mass flux	9495	381	27	moisture	Annual	Balascio and Bradley (2012)	140	170	70	
GeoB12605_3	−6	39	−195	Marine	Mg/Ca	9710	1335	28	SST	Annual	Kuhnert et al. (2014)	180	90		
GeoB3313−1	−41	−74	−852	Marine	$d^{18}O$	6953	13	46	SST	Annual	Lamy et al. (2002)	610	370	310	y
GeoB5901_2	36	−7	−574	Marine	alkenone	9920	1130	20	SST	Annual	Kim et al. (2004)	130			

(*continued on next page*)

Table 4 (*continued*)

Record	Lat (°)	Lon (°)	Elev (m)	Archive	Proxy	Max age	Min age)	dt (yr)	Variable	Seasonality	Citation	Period length (yr)			QC com
GIK17940_2	20	117	−1727	Marine	$d^{18}O$	41107	14	28	SST	Annual	Pelejero et al. (1999)	570	400	330	
GiK18515_3	−4	119	−688	Marine	Mg/Ca	26421	214	50	SST	Annual	Schröder et al. (2016)	850	500	85	y
GIK23258−2/3	75	14	−1768	Marine	$d^{18}O$.foram	13987	0	35	SST	Summer	Sarnthein et al. (2003)	240	290	140	
GISP2	73	−38	3216	Ice	$d^{18}O$.ice	49981	95	31	Air temp	Annual	Alley (2000)	950	150	90	y
Graham	45	−77	381	Lake	pollen	10980	1	39	Air temp	Summer	Fuller (1997)	180	80		
Great Basin	38	−117	0	Tree	TRW	4524	−56	1	Air temp	Summer	Salzer et al. (2014)	110	70		
Grenadier	44	−79	76	Lake	pollen	4631	−27	44	Air temp	Annual	McAndrews (1984)	270	140		
GRIP	72	−38	3230	Ice	$d^{18}O$.ice	32380	−20	20	Air temp	Annual	Vinther et al. (2006)	90			
Hallet Lake	62	−146	1128	Lake	OM, BSi	7913	−52	35	Air temp	Summer	McKay and Kaufman (2009)	None			
Haukdalsvatn	65	−21	32	Lake	$d^{13}C$.bulk	10000	−1	3	Air temp	Summer	Geirsdóttir et al. (2013)	240	140		y
High	45	−77	192	Lake	pollen	10566	0	41	Air temp	Winter	Fuller (1997)	130	90		
Holzmaar	50	7	425	Lake	pollen	10881	−23	40	Air temp	Winter	Litt et al. (2009)	170	240	110	y
Hurleg lake	37	97	2817	Lake	alkenones	8661	481	42	Air temp	Summer	Zhao et al. (2013)	110	80		
Hvitarvatn	65	−20	422	Lake	BSi, $d^{13}C$.bulk	10181	−38	6	Air temp	Summer	Larsen et al. (2012)	330	260	170	y
Jinchuan Peat Bog	42	126	600	Peat	$d^{18}O$	5752	20	24	Air temp	Summer	Yu (2013)	240	120	80	
JR01	70	−95	120	Lake	chironomids	6916	−24	43	LST	Summer	Fortin and Gajewski (2016)	240	170	110	
Kaite Cobre Mayor	43	−4	1173	Speleothem	$d^{13}C$	3899	−50	3	Air temp	Annual	Martin-Chivelet et al. (2011)	None			
Kinderlinskaya Cave	54	57	240	Speleothem	$d^{18}O$	11704	−50	9	Air temp	Winter	Baker et al. (2017)	90			
KNR166_JPC26	24	−83	−546	Marine	Mg/Ca	34490	640	10	SST	Annual	Schmidt and Stieglitz (2011)	None			
KNR166_JPC51	24	−83	−198	Marine	$d^{18}O$	9149	1488	25	SST	Annual	Schmidt et al. (2012)	200	100	70	
KNR195_5_CDH23	−4	−81	−370	Marine	alkenones	14094	1273	33	SST	Annual	Bova et al. (2015)	90			
Komsomolskaia	−74	97	3499	Ice	dD	14934	0	17	Air temp	Annual	Ciais et al. (1992)	550	370	250	
Kortlandamossen1	60	12	112	Peat	humification index	9759	226	45	moisture	Annual	Borgmark and Wastegård (2008)	380	300		
Kurupa Lake	68	−155	920	Lake	chlorophyll	5594	−53	3	Air temp	Summer	Boldt et al. (2015)	440			
Lac Aurelie	50	−74	440	Lake	chironomids	8282	−19	47	Air temp	Summer	Bajolle et al. (2018)	280	240	140	
lapland	69	25		Tree	width	7450	−55	1	Air temp	July	Helama et al. (2010)	80	260	310	
Le Grand Lemps	45	5	680	Peat	pollen	10964	−4	28	Air temp	Summer	Beaulieu (2006)	560	390		
Leviathan	38	−116	2400	Speleothem	$d^{18}O$	13308	−60	5	Air temp	Annual	Lachniet et al. (2014)	430	240	150	
Lingreville	49	−2	5	Marine	pollen	4000	−34	29	Air temp	Annual	Billard et al. (1995)	340			y
LO09−14	59	−30		Marine	diatoms	10976	368	32	SST	August	Berner et al. (2008)	230	150	190	
Lone Spruce Pond	60	−159	135	Lake	BSi	14524	−5	40	Air temp	growing	Kaufman et al. (2012)	140			
M39008_3	36	−7	−577	Marine	$d^{18}O$	21497	875	38	SST	Annual	Eynaud et al. (2009)	None			
M40-4-SL78	37	13	−470	Marine	alkenones	11380	20	40	SST	Annual	Emeis and Dawson (2003)	420	320	260	y
MD02_2515	27	−112	−881	Marine	GDGT	24989	6825	47	SST	Annual	McClymont et al. (2012)	160	60	100	
MD03_2707	3	9	−1295	Marine	$d^{18}O$	155420	360	40	SST	Annual	Weldeab et al. (2007)	140	190	90	
MD95−2011	67	8	−1048	Marine	d18O.foram	6026	−45	15	SST	August	Berner et al. (2010)	720	60		y
MD97_2141	9	121	−3633	Marine	$d^{18}O$	146440	4286	44	SST	Annual	Rosenthal et al. (2003)	300	150	90	
MD98_2161	−5	117	−1185	Marine	$d^{18}O$	25046	−6	34	SST	Annual	Fan et al. (2018)	370	300	240	
MD98_2176	−5	133	−2382	Marine	$d^{18}O$	20333	126	43	SST	Annual	Stott et al. (2007)	280	360	190	
MD98_2178	4	119	−1984	Marine	Mg/Ca	25014	1630	24	SST	Annual	Fan et al. (2018)	210	90	110	
MD98_2181	6	126	−2114	Marine	Mg/Ca	21869	3	36	SST	Annual	Stott et al. (2007)	280	200	150	y
MD99−2269	67	−21		Marine	diatoms	11477	−16	37	SST	August	Justwan et al. (2008)	470	250	190	y
MD99−2284	62	1	−1500	Marine	foraminifera	11996	998	24	SST	Annual	Risebrobakken et al. (2003)	420	320	250	y
Meerfelder Maar	50	7	336,5	Lake	pollen	10990	163	20	Air temp	Annual	Litt et al. (2009)	150	80		y
Midden Cluster 1	38	−110	1835	Midden	macrofossils	15211	0	27	Air temp	Annual	Harbert and Nixon (2018)	900			y
Milandre Cave	47	7	491	Speleothem	dD	13923	−20	35	Air temp	Annual	Affolter et al. (2019)	280	210	170	
Minnetonka Cave	42	−112	2347	Speleothem	$d^{18}O$	11122	7	7	Air temp	Winter	Lundeen et al. (2013)	None			y
Mjáuvötn	62	−7	200	Lake	XRF, $d^{13}C$	11611	−40	13	Air temp	Annual	Olsen et al. (2010)	210	180	130	
Moose Lake	61	−144	437	Lake	chironomids	6008	−20	47	Air temp	July	Clegg et al. (2010)	280	180	60	
MSM5/5−723−2	79	5	−1349	Marine	IP25	7010	180	35	Sea ice	Spring	Müller et al. (2012)	290	180		
MV99_PC14	25	−113	−541	Marine	Mg/Ca	13812	2222	42	SST	Annual	Marchitto et al. (2010)	740	180	270	
N14	60	−44	101	Lake	BSi	14377	320	22	Precipitation	Annual	Andresen et al. (2004b)	110			
Nattmålsvatn	69	17	170	Lake	MS	10956	1101	23	moisture	Winter	Janbu et al. (2011)	None			
NAUJG1-1	67	−52	300	Lake	mineral content	9498	429	13	Air temp	Summer	Willemse and Törnqvist (1999)	110	80		y
Nautajärvi	62	25	103,7	Lake	pollen	8998	51	37	Air temp	Annual	Ojala et al. (2008) Seppä et al. (2009)	400	250	130	y
Nerfloen	62	7	938	Lake	multi-proxy_PC_score	7775	−20	50	moisture	Winter	Vasskog et al. (2012)	430	220		
NGRIP	75	−42	2917	Ice	$d^{18}O$.ice	41700	−40	20	Air temp	Annual	Vinther et al. (2006)	120	70		y
OregonCaves	42	−123	1390	Speleothem	$d^{18}O$	7992	234	3	Air temp	Winter	Ersek et al. (2012)	None			y
P1003	64	5	−875	Marine	$d^{18}O$.foram	7881	−48	5	SST	JAS	Sejrup et al. (2011)	900	60		
P1B3	74	−163	−201	Marine	dinocyst	9626	126	50	SST	Summer	de Anne de Vernal et al. (2005)	650	250		
Path Lake	44	−65	15	Lake	pollen	9121	7	43	Air temp	Annual	Neil et al. (2014)	160	140	290	
PC6	40	144	−2215	Marine	alkenones	27018	325	41	SST	Annual	Minoshima et al. (2007)	160	120	90	

Table 4 (*continued*)

Record	Lat (°)	Lon (°)	Elev (m)	Archive	Proxy	Max age	Min age)	dt (yr)	Variable	Seasonality	Citation	Period length (yr)			QC com
Penny Ice Cap	67	−67	1900	Ice	$d^{18}O$.ice	11787	−33	10	Air temp	Annual	Fisher et al. (1998)	120	80		
Plateau Remote	−84	43	3330	Ice	$d^{18}O$	3955	5	10	Air temp	Annual	Mosley-Thompson (1996)	240			
Praz Rodet	47	6	1040	Peat	pollen	10680	−43	43	Air temp	Winter	Shotyk et al. (1997)	90			
Renland	71	−27	2350	Ice	$d^{18}O$.ice	11650	−10	20	Air temp	Annual	Johnsen et al. (1992)	130	80		
Rystad 1	68	14	40	Peat	humification index	8793	−158	30	moisture	Annual	Vorre et al. (2012)	560	340	160	
Saegistalsee	47	8	1940	Lake	pollen	8948	−41	35	Air temp	Annual	Wick et al. (2003)	380	230	170	
Sahara Sand Wetland	48	88	2450	Peat	$d^{13}C$	11030	−25	37	Air temp	Summer	Rao et al. (2019)	390	230	180	
Sellevollmyra	69	16	0,75	Peat	humification index	6852	455	50	moisture	Annual	Vorren et al. (2007)	210	170		
SFL-1	67	−50	247	Lake	OM	7400	12	12	Air temp	Summer	Willemse and Törnqvist (1999)	220	110	160	
Sharkey	45	−93	308	Lake	pollen	13038	634	31	Air temp	Annual	Shuman and Marsicek (2016)	130	90		
Siple Dome A	−82	−149	621	Ice	melt layer	11705	1	1	Air temp	Summer	Das and Alley (2008)	650	280		
SO189_039 KL	−1	100	−517	Marine	$d^{18}O$	45330	410	50	SST	Annual	Mohtadi et al. (2014)	420	330	190	
SO90_56 KA	25	66	−695	Marine	alkenones	4883	6	17	SST	Annual	Doose-Rolinski et al. (2001)	420	320	250	y
SO90_63 KA	25	66	−316	Marine	$d^{18}O$	12754	−40	13	SST	Annual	Staubwasser et al. (2002)	90			
South Island	−42	172	990	Speleothem	$d^{18}O$	29876	508	25	SST	Annual	Williams et al. (2005)	240	300	160	y
Spannagel	47	12	2524	Speleothem	$d^{18}O$	9931	−13	2	Air temp	Annual	Fohlmeister et al. (2013)	60			y
SS1381	67	−51	196	Lake	OM.flux, mineral.flux	8429	46	48	moisture	Annual	Anderson et al. (2012)	340	210	180	
Starvatn	62	−7	94	Lake	flux grains, BSi	11077	1521	43	Air temp	Winter	Andresen et al. (2004a, 2004b)	530	290	200	
Søylegrotta	67	14	280	Speleothem	$d^{18}O$	9955	137	42	Air temp	Annual	Lauritzen and Lundberg (1999)	750	550	110	
TALDICE	−73	159	2315	Ice	d18O	12015	−41	18	Air temp	Annual	Mezgec et al. (2017)	180	100	60	
TN057−17	−50	6	−3700	Marine	diatom	12563	0	45	SST	Summer	Nielsen et al. (2004)	420	320	250	y
Torneträsk	68	20	400	Tree	width	7356	−47	1	Air temp	JJA	Grudd et al. (2002)	310	420	250	
Unit Lake	59	−97	294	Lake	ARM/IRM	8752	−61	44	moisture	Annual	Camill et al. (2012)	None			
Vikjordavatnet	68	14	23	Lake	OM.flux	11643	355	42	Air temp	Annual	Balascio and Bradley (2012)	180	140	310	
Vostok	−79	108	3488	Ice	dD	9840	0	20	Air temp	Annual	Vimeux et al. (2002)	250	120	90	y
WAIS Divide	−79	−112	1806	Ice	hybrid-ice	67771	−56	2	Air temp	Annual	Cuffey et al. (2016)	640	400		
Wilder See beim Ruhestein	49	8	910	Lake	pollen	9644	387	30	Air temp	Annual	Rösch (2009)	260	210	130	
Wolverine Lake	67	−159		Lake	MAR	7407	24	33	moisture	Annual	Mann (2002)	60			

References

Affolter, Stéphane, Häuselmann, Anamaria, Dominik Fleitmann, R., 2019. Lawrence Edwards, Hai Cheng and Markus Leuenberger. *Central Europe temperature constrained by speleothem fluid inclusion water isotopes over the past 14,000 years*. Sci. Adv. 5 (6), eaav3809. https://doi.org/10.1126/sciadv.aav3809.

Akima, Hiroshi, 1970. A new method of interpolation and smooth curve fitting based on local procedures. J. ACM 17 (4), 589–602. https://doi.org/10.1145/321607.321609.

Allan, Estelle, Anne de Vernal, Faurschou Knudsen, Mads, Hillaire-Marcel, Claude, Moros, Matthias, Ribeiro, Sofia, Ouellet-Bernier, Marie-Michèle, Seidenkrantz, Marit-Solveig, 2018. Late holocene sea surface instabilities in the disko bugt area, west Greenland, in phase with δ18O oscillations at camp century. Paleoceanogr. Paleoclimatol. 33 (2), 227–243. https://doi.org/10.1002/2017PA003289. ISSN 2572-4517.

Alley, R.B., 2000. The Younger Dryas cold interval as viewed from central Greenland. Quat. Sci. Rev. 19 (1–5), 213–226. https://doi.org/10.1016/S0277-3791(99)00062-1.

Borgmark, Anders, Wastegård, Stefan, 2008. Regional and local patterns of peat humification in three raised peat bogs in Värmland, south-central Sweden. GFF 130 (3), 161–176. https://doi.org/10.1080/11035890809453231.

Andersen, K.K., Azuma, N., Barnola, J.-M., Bigler, M., Biscaye, P., Caillon, N., Chappellaz, J., Clausen, H.B., Dahl-Jensen, D., Fischer, H., Flückiger, J., Fritzsche, D., Fujii, Y., Goto-Azuma, K., Grønvold, K., Gundestrup, N.S., Hansson, M., Huber, C., Hvidberg, C.S., Johnsen, S.J., 2004a. High-resolution record of Northern Hemisphere climate extending into the last interglacial period. Nature 431 (7005), 147–151. ISSN 00280836.

Anderson, N.J., Liversidge, A.C., McGowan, S., Jones, M.D., 2012. Lake and catchment response to Holocene environmental change: spatial variability along a climate gradient in southwest Greenland. J. Paleolimnol. 48 (1), 209–222. https://doi.org/10.1007/s10933-012-9616-3. ISSN 1573-0417.

Andresen, Camilla S., Björck, Svante, Bennike, Ole, Bond, Gerard, 2004b. Holocene climate changes in southern Greenland: evidence from lake sediments. J. Quat. Sci. 19 (8), 783–795. https://doi.org/10.1002/jqs.886.

Anne de Vernal, Hillaire-Marcel, Claude, Darby, Dennis A., 2005. Variability of sea ice cover in the chukchi sea (western Arctic Ocean) during the holocene. Paleoceanography 20 (4). https://doi.org/10.1029/2005PA001157.

Asmerom, Yemane, Polyak, Victor, Burns, Stephen, Rassmussen, Jessica, 2007. Solar forcing of Holocene climate: new insights from a speleothem record, southwestern United States. Geology 35 (1), 1–4. https://doi.org/10.1130/G22865A.1. ISSN 0091-7613.

Bader, Jürgen, Jungclaus, Johann, Krivova, Natalie, Lorenz, Stephan, Maycock, Amanda, Raddatz, Thomas, Schmidt, Hauke, Toohey, Matthew, Wu, Chi-Ju, Martin, Claussen, 2020. Global temperature modes shed light on the Holocene temperature conundrum. Nat. Commun. 11 (1), 4726. https://doi.org/10.1038/s41467-020-18478-6. ISSN 2041-1723.

Bae, Junghyun, Chatzidakis, Stylianos, 2022. Fieldable muon spectrometer using multi-layer pressurized gas Cherenkov radiators and its applications. Sci. Rep. 12 (1), 2559. https://doi.org/10.1038/s41598-022-06510-2. ISSN 2045-2322.

Bajolle, Lisa, Larocque-Tobler, Isabelle, Gandouin, Emmanuel, Lavoie, Martin, Bergeron, Yves, Ali, Adam A., 2018. Major postglacial summer temperature changes in the central coniferous boreal forest of Quebec (Canada) inferred using chironomid assemblages. J. Quat. Sci. 33 (4), 409–420. https://doi.org/10.1002/jqs.3022.

Baker, Jonathan L., Lachniet, Matthew S., Chervyatsova, Olga, Asmerom, Yemane, Polyak, Victor J., 2017. Holocene warming in western continental Eurasia driven by glacial retreat and greenhouse forcing. Nat. Geosci. 10 (6), 430–435. https://doi.org/10.1038/ngeo2953. ISSN 1752-0908.

Balascio, Nicholas L., Bradley, Raymond S., 2012. Evaluating Holocene climate change in northern Norway using sediment records from two contrasting lake systems. J. Paleolimnol. 48 (1), 259–273. https://doi.org/10.1007/s10933-012-9604-7. ISSN 1573-0417.

Beaulieu, Clerc, 2006. Recherches pollenanalytiques sur la paleocologie tardiglaciaire et holocone du Bas-Dauphine. Atelier national de reproduction des theses, Grenoble.

Beer, Jürg, 2000. Long-term indirect indices of solar variability. Space Sci. Rev. 94 (1), 53–66. https://doi.org/10.1023/A:1026778013901. ISSN 1572-9672.

Beer, Jürg, Baumgartner, Stephan T., Dittrich-Hannen, Beate, Hauenstein, Jürg, Kubik, Peter, Lukasczyk, Christian, Werner, Mende, Stellmacher, Rita, Suter, Martin, 1994. Solar variability traced by cosmogenic isotopes. Int. Astron. Union Circular 143, 291–300. https://doi.org/10.1017/S0252921100024799. ISSN 0252-9211.

Belt, Simon T., Vare, Lindsay L., Massé, Guillaume, Manners, Hayley R., Price, John C., MacLachlan, Suzanne E., Andrews, John T., Schmidt, Sabine, 2010. Striking similarities in temporal changes to spring sea ice occurrence across the central Canadian Arctic Archipelago over the last 7000 years. Quat. Sci. Rev. 29 (25), 3489–3504. https://doi.org/10.1016/j.quascirev.2010.06.041. ISSN 0277-3791.

Berger, AndréL., 1978. Long-term variations of caloric insolation resulting from the earth's orbital elements. Quat. Res. 9 (2), 139–167. https://doi.org/10.1016/0033-5894(78)90064-9. ISSN 0033-5894.

Berger, A., Loutre, M.F., 1991. Insolation values for the climate of the last 10 million years. Quat. Sci. Rev. 10 (4), 297–317. https://doi.org/10.1016/0277-3791(91)90033-Q. ISSN 0277-3791.

Berner, K.S., Koç, N., Divine, D., Godtliebsen, F., Moros, M., 2008. A decadal-scale Holocene sea surface temperature record from the subpolar North Atlantic constructed using diatoms and statistics and its relation to other climate parameters. Paleoceanography 23 (2). https://doi.org/10.1029/2006PA001339.

Berner, K.S., Koç, N., Godtliebsen, F., 2010. High frequency climate variability of the Norwegian Atlantic current during the early Holocene period and a possible connection to the Gleissberg cycle. Holocene 20 (2), 245–255. https://doi.org/10.1177/0959683609350391.

Billard, Cyrille, Clet-Pellerin, Martine, Lautridou, Jean Pierre, Giffault, Michèle, 1995. Un site protohistorique littoral dans le havre de la Vanlée à Lingreville et Bricqueville-sur-Mer (Manche). Rev. Archéol. Ouest 12, 73–110. https://doi.org/10.3406/rao.1995.1026.

Binka, K., Madeyska, T., Marciniak, B., Seroczynska, K., Wieckowski, K., 1988. Bledowo Lake (central Poland): history of vegetation and lake development during the last 12 kyr. Bull Acad Pol. Sci 36, 147–158.

Boldt, Brandon R., Kaufman, Darrell S., McKay, Nicholas P., Briner, Jason P., 2015. Holocene summer temperature reconstruction from sedimentary chlorophyll content, with treatment of age uncertainties, Kurupa Lake, Arctic Alaska. Holocene 25 (4), 641–650. https://doi.org/10.1177/0959683614565929. ISSN 0959-6836.

Bond, Gerard, Kromer, Bernd, Beer, Juerg, Muscheler, Raimund, Evans, Michael N., Showers, William, Hoffmann, Sharon, Lotti-Bond, Rusty, Hajdas, Irka, Bonani, Georges, 2001. Persistent solar influence on North Atlantic climate during the holocene. Science 294 (5549), 2130–2136. ISSN 00368075, 10959203.

Bova, Samantha, Herbert, Timothy, Rosenthal, Yair, Kalansky, Julie, Altabet, Mark, Chazen, Caitlin, Mojarro, Angel, Zech, Jana, 2015. Links between eastern equatorial pacific stratification and atmospheric CO2 rise during the last deglaciation. Paleoceanography 30. https://doi.org/10.1002/2015PA002816.

Braconnot, P., Zhu, D., Marti, O., Servonnat, J., 2019. Strengths and challenges for transient Mid- to Late Holocene simulations with dynamical vegetation. Clim. Past 15 (3), 997–1024. https://doi.org/10.5194/cp-15-997-2019.

Brovkin, V., Lorenz, S., Raddatz, T., Ilyina, T., Stemmler, I., Toohey, M., Claussen, M., 2019. What was the source of the atmospheric CO2 increase during the Holocene? Biogeosciences 16 (13), 2543–2555. https://doi.org/10.5194/bg-16-2543-2019.

Bunn, Andy, Korpela, Mikko, Franco, Biondi, Campelo, Filipe, Mérian, Pierre, Qeadan, Fares, Zang, Christian, Allan, Buras, Jacob, Cecile, Mudelsee, Manfred, Schulz, Michael, Stefan, Klesse, Frank, David, Ronald, Visser, 2021. Package 'DplR' - Dendrochronology Program Library in R. https://cran.r-project.org/web/packages/dplR/dplR.pdf. accessed: 16-02-2022.

Camill, Philip, Umbanhowar, Charles E., Geiss, Christoph, Hobbs, William O., Edlund, Mark B., Avery Cook, Shinneman, Dorale, Jeffrey A., Lynch, Jason, 2012. Holocene climate change and landscape development from a low-Arctic tundra lake in the western Hudson Bay region of Manitoba, Canada. J. Paleolimnol. 48 (1), 175–192. https://doi.org/10.1007/s10933-012-9619-0. ISSN 1573-0417.

CESM Software Engineering Group CSEG, 2020. CESM1.0.z User's Guide. https://www.cesm.ucar.edu/models/cesm1.0/cesm/cesm_doc_1_0_6/ug.pdf. Accessed: 23-04-2022.

Ciais, P., Petit, J.R., Jouzel, J., Lorius, C., Barkov, N.I., Lipenkov, V., Nicolaïev, V., 1992. Evidence for an early Holocene climatic optimum in the Antarctic deep ice-core record. Clim. Dynam. 6 (3), 169–177. https://doi.org/10.1007/BF00193529. ISSN 1432-0894.

Clegg, B.F., Clarke, G.H., Chipman, M.L., Chou, M., Walker, I.R., Tinner, W., Hu, F.S., 2010. Six millennia of summer temperature variation based on midge analysis of lake sediments from Alaska. Quat. Sci. Rev. 29 (23–24), 3308–3316. https://doi.org/10.1016/j.quascirev.2010.08.001.

Crosta, X., Debret, M., Denis, D., Courty, M.A., Ther, O., 2007. Holocene long- and short-term climate changes off Adélie Land, East Antarctica. G-cubed 8 (11). https://doi.org/10.1029/2007GC001718.

Cuffey, Kurt M., Gary, D Clow, Steig, Eric J., Buizert, Christo, Fudge, T.J., Koutnik, Michelle, Edwin D Waddington, Richard B Alley, Severinghaus, Jeffrey P., 2016. Deglacial temperature history of West Antarctica. Proc. Natl. Acad. Sci. USA 113 (50), 14249–14254. https://doi.org/10.1073/pnas.1609132113. ISSN 0027-8424.

Czymzik, Markus, Brauer, Achim, Peter, Dulski, Plessen, Birgit, Naumann, Rudolf, Von Grafenstein, Ulrich, Scheffler, Raphael, 2013. Orbital and solar forcing of shifts in Mid- to Late Holocene flood intensity from varved sediments of prealpine Lake Ammersee (southern Germany). Quat. Sci. Rev. 61, 96–110. https://doi.org/10.1016/j.quascirev.2012.11.010.

Dallmeyer, A., Claussen, M., Lorenz, S.J., Shanahan, T., 2020. The end of the African humid period as seen by a transient comprehensive Earth system model simulation of the last 8000 years. Clim. Past 16 (1), 117–140. https://doi.org/10.5194/cp-16-117-2020.

Das, Sarah B., Alley, Richard B., 2008. Rise in frequency of surface melting at Siple Dome through the Holocene: evidence for increasing marine influence on the climate of West Antarctica. J. Geophys. Res. Atmos. 113 (D2). https://doi.org/10.1029/2007JD008790.

De Jager, C., 2005. Solar forcing of climate. 1: solar variability. Space Sci. Rev. 120 (3), 197–241. https://doi.org/10.1007/s11214-005-7046-5. ISSN 1572-9672.

Dee, S., Emile-Geay, J., Evans, M.N., Allam, A., Steig, E.J., Thompson, D.M., 2015. PRYSM: an open-source framework for PRoxY System Modeling, with applications to oxygen-isotope systems. J. Adv. Model. Earth Syst. 7 (3), 1220–1247. https://doi.org/10.1002/2015MS000447. ISSN 1942-2466.

Dee, S.G., Parsons, L.A., Loope, G.R., Overpeck, J.T., Ault, T.R., Emile-Geay, J., 2017. Improved spectral comparisons of paleoclimate models and observations via proxy system modeling: implications for multi-decadal variability. Earth Planet Sci. Lett. 476 (34–46). https://doi.org/10.1016/j.epsl.2017.07.036. ISSN 0012-821X.

Delworth, Thomas L., Zeng, Fanrong, 2012. Multicentennial variability of the Atlantic meridional overturning circulation and its climatic influence in a 4000 year simulation of the GFDL CM2.1 climate model. Geophys. Res. Lett. 39 (13). https://doi.org/10.1029/2012GL052107. ISSN 0094-8276.

Doose-Rolinski, Heidi, Rogalla, Ulf, Scheeder, Georg, Lückge, Andreas, Ulrich von Rad, 2001. High-resolution temperature and evaporation changes during the late holocene in the northeastern arabian sea. Paleoceanography 16 (4), 358–367. https://doi.org/10.1029/2000PA000511.

Emeis, Kay-Christian, Dawson, Alastair G., 2003. Holocene palaeoclimate records over europe and the north atlantic. Holocene 13 (3), 305–309. https://doi.org/10.1191/0959683603hl622ed.

Ersek, Vasile, Clark, Peter U., Mix, Alan C., Cheng, Hai, Edwards, R Lawrence, 2012. Holocene winter climate variability in mid-latitude western North America. Nat. Commun. 3 (1), 1219. https://doi.org/10.1038/ncomms2222. ISSN 2041-1723.

Esri, 2022. World Imagery. https://www.arcgis.com/home/item.html?id=10df2279f9684e4a9f6a7f08febac2a9. Accessed: 10-05-2022.

Evans, M.N., Tolwinski-Ward, S.E., Thompson, D.M., Anchukaitis, K.J., 2013. Applications of proxy system modeling in high resolution paleoclimatology. Quat. Sci. Rev. 76 (16–28). https://doi.org/10.1016/j.quascirev.2013.05.024. ISSN 0277-3791.

Eynaud, Frédérique, de Abreu, Lúcia, Voelker, Antje, Schönfeld, Joachim, Salgueiro, Emilia, Turon, Jean-Louis, Penaud, Aurélie, Toucanne, Samuel, Naughton, Filipa, Sánchez Goñi, María Fernanda, Bruno, Malaizé, Cacho, Isabel, 2009. Position of the Polar Front along the western Iberian margin during key cold episodes of the last 45 ka. G-cubed 10 (7). https://doi.org/10.1029/2009GC002398.

Eyring, V., Bony, S., Meehl, G.A., Senior, C.A., Stevens, B., Stouffer, R.J., Taylor, K.E., 2016. Overview of the coupled model Intercomparison Project phase 6 (CMIP6) experimental design and organization. Geosci. Model Dev. (GMD) 9 (5), 1937–1958. https://doi.org/10.5194/gmd-9-1937-2016.

Fan, Weijia, Jian, Zhimin, Chu, Zhihui, Dang, Haowen, Wang, Yue, Bassinot, Franck, Han, Xiqiu, Bian, Yeping, 2018. Variability of the Indonesian throughflow in the makassar strait over the last 30 ka. Sci. Rep. 8 (1), 5678. https://doi.org/10.1038/s41598-018-24055-1. ISSN 2045-2322.

Fernández-Donado, L., González-Rouco, J.F., Raible, C.C., Ammann, C.M., Barriopedro, D., García-Bustamante, E., Jungclaus, J.H., Lorenz, S.J., Luterbacher, J., Phipps, S.J., Servonnat, J., Swingedouw, D., Tett, S.F.B., Wagner, S., Yiou, P., Zorita, E., 2013. Large-scale temperature response to external forcing in simulations and reconstructions of the last millennium. Clim. Past 9 (1), 393–421. https://doi.org/10.5194/cp-9-393-2013.

Finney, Bruce, Bigelow, Nancy, Barber, Valerie, Edwards, Mary, 2012. Holocene climate change and carbon cycling in a groundwater-fed, boreal forest lake: dune Lake, Alaska. J. Paleolimnol. 48. https://doi.org/10.1007/s10933-012-9617-2.

Fisher, D.A., Koerner, R.M., Paterson, W.S.B., Dansgaard, W., Gundestrup, N., Reeh, N., 1983. Effect of wind scouring on climatic records from ice-core oxygen-isotope profiles. Nature 301 (5897), 205–209. https://doi.org/10.1038/301205a0. ISSN 1476-4687.

Fisher, David A., Koerner, Roy M., Bourgeois, Jocelyne C., Zielinski, Greg, Cameron, Wake, Hammer, Claus U., Clausen, H.B., Gundestrup, N., Johnsen, Sigfus, Goto-Azuma, Kumiko, Hondoh, Takeo, Blake, Erik, Gerasimoff, Mike, 1998. Penny ice cap cores, baffin island, Canada, and the wisconsinan foxe dome connection: two states of hudson bay ice cover. Science 279 (5351), 692–695. ISSN 00368075, 10959203.

Flückiger, Jacqueline, Monnin, Eric, Stauffer, Bernhard, Schwander, Jakob, Stocker, Thomas F., Chappellaz, Jérôme, Raynaud, Dominique, Barnola, Jean-Marc, 2002. High-resolution Holocene N2O ice core record and its relationship with CH4 and CO2. Global Biogeochem. Cycles 16 (1), 10–11. https://doi.org/10.1029/2001GB001417. –10–8.

Fohlmeister, Jens, Vollweiler, Nicole, Spötl, Christoph, Mangini, Augusto, 2013. COMNISPA II: update of a mid-European isotope climate record, 11 ka to present. Holocene 23 (5), 749–754. https://doi.org/10.1177/0959683612465446.

Fortin, Marie-Claude, Gajewski, Konrad, 2016. Multiproxy paleoecological evidence of holocene climatic changes on the boothia peninsula, Canadian arctic. Quat.

Res. 85 (3), 347–357. https://doi.org/10.1016/j.yqres.2016.02.003.
Friedrich, T., Timmermann, A., Menviel, L., Timm, O Elison, Mouchet, A., Roche, D.M., 2010. The mechanism behind internally generated centennial-to-millennial scale climate variability in an earth system model of intermediate complexity. Geosci. Model Dev. (GMD) 3 (2), 377–389. https://doi.org/10.5194/gmd-3-377-2010.
Fuller, Janice L., 1997. Holocene forest dynamics in southern Ontario, Canada: fine-resolution pollen data. Can. J. Bot. 75 (10), 1714–1727. https://doi.org/10.1139/b97-886.
Gavin, Daniel G., Henderson, Andrew C.G., Karlyn, S Westover, Fritz, Sherilyn C., Walker, Ian R., Leng, Melanie J., Hu, Feng Sheng, 2011. Abrupt Holocene climate change and potential response to solar forcing in western Canada. Quat. Sci. Rev. 30 (9), 1243–1255. https://doi.org/10.1016/j.quascirev.2011.03.003. ISSN 0277-3791.
Geirsdóttir, Áslaug, Miller, Gifford H., Larsen, Darren J., Ólafsdóttir, Sædís, 2013. Abrupt Holocene climate transitions in the northern North Atlantic region recorded by synchronized lacustrine records in Iceland. Quat. Sci. Rev. 70 (48–62). https://doi.org/10.1016/j.quascirev.2013.03.010. ISSN 0277-3791.
Gordon, C., Cooper, C., Senior, C.A., Banks, H., Gregory, J.M., Johns, T.C., Mitchell, J.F.B., Wood, R.A., 2000. The simulation of SST, sea ice extents and ocean heat transports in a version of the Hadley Centre coupled model without flux adjustments. Clim. Dynam. 16 (2), 147–168. https://doi.org/10.1007/s003820050010. ISSN 1432-0894.
Grudd, H., Briffa, K.R., Karlén, W., Bartholin, T.S., Jones, P.D., Kromer, B., 2002. A 7400-year tree-ring chronology in northern Swedish Lapland: natural climatic variability expressed on annual to millennial timescales. Holocene 12 (6), 657–665. https://doi.org/10.1191/0959683602hl578rp.
Harbert, R.S., Nixon, K.C., 2018. Quantitative late quaternary climate reconstruction from plant macrofossil communities in Western North America. Open Quat. 4. https://doi.org/10.5334/oq.46.
Hawkins, Ed, Sutton, Rowan, 2007. Variability of the Atlantic thermohaline circulation described by three-dimensional empirical orthogonal functions. Clim. Dynam. 29 (7), 745–762. https://doi.org/10.1007/s00382-007-0263-8. ISSN 1432-0894.
Helama, S., Fauria, M.M., Mielikäinen, K., Timonen, M., Eronen, M., 2010. Sub-Milankovitch solar forcing of past climates: mid and late holocene perspectives. Bull. Geol. Soc. Am. 122 (11–12), 1981–1988. https://doi.org/10.1130/B30088.1.
Hopcroft, Peter O., Valdes, Paul J., 2021. Paleoclimate-conditioning reveals a North Africa land & atmosphere tipping point. Proc. Natl. Acad. Sci. USA 118 (45), e2108783118. https://doi.org/10.1073/pnas.2108783118.
Hopcroft, Peter, Valdes, Paul, 2022. Green Sahara tipping points in transient climate model simulations of the Holocene. Environ. Res. Lett. https://doi.org/10.1088/1748-9326/ac7c2b.
Hörner, Tanja, Stein, Ruediger, Fahl, Kirsten, 2017. Evidence for Holocene centennial variability in sea ice cover based on IP25 biomarker reconstruction in the southern Kara Sea (Arctic Ocean). Geo Mar. Lett. 37. https://doi.org/10.1007/s00367-017-0501-y.
Hurtt, G.C., Chini, L.P., Frolking, S., Betts, R.A., Feddema, J., Fischer, G., Fisk, J.P., Hibbard, K., Houghton, R.A., Janetos, A., Jones, C.D., Kindermann, G., Kinoshita, T., Kees Klein Goldewijk, K Riahi, Shevliakova, E., Smith, S., Stehfest, E., Thomson, A., Thornton, P., van Vuuren, D.P., Wang, Y.P., 2011. Harmonization of land-use scenarios for the period 1500–2100: 600 years of global gridded annual land-use transitions, wood harvest, and resulting secondary lands. Climatic Change 109 (1), 117. https://doi.org/10.1007/s10584-011-0153-2. ISSN 1573-1480.
Janbu, Aina Dahlø, Paasche, Øyvind, Talbot, Michael R., 2011. Paleoclimate changes inferred from stable isotopes and magnetic properties of organic-rich lake sediments in Arctic Norway. J. Paleolimnol. 46 (1), 29. https://doi.org/10.1007/s10933-011-9512-2. ISSN 1573-0417.
Jiang, Weimin, Gastineau, Guillaume, Codron, Francis, 2021. Multicentennial variability driven by salinity exchanges between the atlantic and the Arctic Ocean in a coupled climate model. J. Adv. Model. Earth Syst. 13 (3), e2020MS002366. https://doi.org/10.1029/2020MS002366. ISSN 1942-2466.
Johnsen, S.J., Clausen, H.B., Dansgaard, W., Fuhrer, K., Gundestrup, N., Hammer, C.U., Iversen, P., Jouzel, J., Stauffer, B., Steffensen, J.P., 1992. Irregular glacial interstadials recorded in a new Greenland ice core. Nature 359 (6393), 311–313. https://doi.org/10.1038/359311a0. ISSN 1476-4687.
Joos, Fortunat, Spahni, Renato, 2008. Rates of change in natural and anthropogenic radiative forcing over the past 20,000 years. Proc. Natl. Acad. Sci. USA 105 (5), 1425–1430. https://doi.org/10.1073/pnas.0707386105.
Justwan, A., Koç, N., Jennings, A.E., 2008. Evolution of the Irminger and East Icelandic Current systems through the Holocene, revealed by diatom-based sea surface temperature reconstructions. Quat. Sci. Rev. 27 (15–16), 1571–1582. https://doi.org/10.1016/j.quascirev.2008.05.006.
Kageyama, M., Braconnot, P., Harrison, S.P., Haywood, A.M., Jungclaus, J.H., Otto-Bliesner, B.L., Peterschmitt, J.-Y., Abe-Ouchi, A., Albani, S., Bartlein, P.J., Brierley, C., Crucifix, M., Dolan, A., Fernandez-Donado, L., Fischer, H., Hopcroft, P.O., Ivanovic, R.F., Lambert, F., Lunt, D.J., Mahowald, N.M., Peltier, W.R., Phipps, S.J., Roche, D.M., Schmidt, G.A., Tarasov, L., Valdes, P.J., Zhang, Q., Zhou, T., 2018. The PMIP4 contribution to CMIP6 – Part 1: overview and over-arching analysis plan. Geosci. Model Dev. (GMD) 11 (3), 1033–1057. https://doi.org/10.5194/gmd-11-1033-2018.
Kaufman, Darrell, Axford, Yarrow, Anderson, R., Scott, Lamoureux, Schindler, Daniel, Walker, Ian, Werner, A., 2012. A multi-proxy record of the Last Glacial Maximum and last 14,500 years of paleoenvironmental change at Lone Spruce Pond, southwestern Alaska. J. Paleolimnol. 48. https://doi.org/10.1007/s10933-012-9607-4.
Kaufman, Darrell, McKay, Nicholas, Routson, Cody, Erb, Michael, Davis, Basil, Oliver, Heiri, Jaccard, Samuel, Tierney, Jessica, Dätwyler, Christoph, Axford, Yarrow, Brussel, Thomas, Cartapanis, Olivier, Chase, Brian, Dawson, Andria, Anne de Vernal, Engels, Stefan, Jonkers, Lukas, Marsicek, Jeremiah, Moffa-Sánchez, Paola, Morrill, Carrie, Orsi, Anais, Rehfeld, Kira, Saunders, Krystyna, Sommer, Philipp S., Thomas, Elizabeth, Tonello, Marcela, Tóth, Mónika, Vachula, Richard, Andreev, Andrei, Bertrand, Sebastien, Biskaborn, Boris, Bringué, Manuel, Brooks, Stephen, Caniupán, Magaly, Chevalier, Manuel, Cwynar, Les, Emile-Geay, Julien, Fegyveresi, John, Feurdean, Angelica, Walter, Finsinger, Fortin, Marie-Claude, Foster, Louise, Fox, Mathew, Gajewski, Konrad, Grosjean, Martin, Hausmann, Sonja, Heinrichs, Markus, Holmes, Naomi, Ilyashuk, Boris, Elena, Ilyashuk, Juggins, Steve, Khider, Deborah, Karin, Koinig, Langdon, Peter, Larocque-Tobler, Isabelle, Li, Jianyong, Lotter, André, Luoto, Tomi, Mackay, Anson, Magyari, Eniko, Malevich, Steven, Bryan, Mark, Massaferro, Julieta, Vincent, Montade, Nazarova, Larisa, Elena, Novenko, Pařil, Petr, Pearson, Emma, Peros, Matthew, Reinhard, Pienitz, Płóciennik, Mateusz, Porinchu, David, Potito, Aaron, Rees, Andrew, Scott, Reinemann, Roberts, Stephen, Rolland, Nicolas, Salonen, Sakari, 2020. Angela self, heikki Seppä, shyhrete shala, jeannine-marie st-jacques, barbara stenni, liudmila syrykh, pol tarrats, karen taylor, valerie van den Bos, gaute velle, eugene wahl, ian walker, janet wilmshurst, enlou Zhang and snezhana zhilich. *A global database of Holocene paleotemperature records*. Sci. Data 7 (1), 115. https://doi.org/10.1038/s41597-020-0445-3. ISSN 2052-4463. https://www.ncei.noaa.gov/access/paleo-search/study/21171.
Kennett, Douglas J., James P Kennett, Erlandson, Jon M., Cannariato, Kevin G., 2007. Human responses to middle holocene climate change on California's channel islands. Quat. Sci. Rev. 26 (3), 351–367. https://doi.org/10.1016/j.quascirev.2006.07.019. ISSN 0277-3791.
Kim, Jung-Hyun, Rimbu, Norel, Lorenz, Stephan J., Lohmann, Gerrit, Nam, Seung-Il, Schouten, Stefan, Rühlemann, Carsten, Schneider, Ralph R., 2004. North pacific and North atlantic sea-surface temperature variability during the holocene. Quat. Sci. Rev. 23 (20), 2141–2154. https://doi.org/10.1016/j.quascirev.2004.08.010. ISSN 0277-3791.
Kim, Jung-Hyun, Meggers, Helge, Rimbu, Norel, Lohmann, Gerrit, Tim Freudenthal, Müller, Peter J., Schneider, Ralph R., 2007. Impacts of the north atlantic gyre circulation on holocene climate off northwest Africa. Geology 35 (5), 387–390. https://doi.org/10.1130/G23251A.1. ISSN 0091-7613.
Köhler, P., Nehrbass-Ahles, C., Schmitt, J., Stocker, T.F., Fischer, H., 2017. *A 156 kyr smoothed history of the atmospheric greenhouse gases CO_2, CH_4, and N_2O and their radiative forcing*. Earth Syst. Sci. Data 9 (1), 363–387. https://doi.org/10.5194/essd-9-363-2017.
Korjonen, Kaarina Sarmaja, Seppä, Heikki, 2007. Abrupt and consistent responses of aquatic and terrestrial ecosystems to the 8200 cal. yr cold event: a lacustrine record from Lake Arapisto, Finland. Holocene 17 (4), 457–467. https://doi.org/10.1177/0959683607077020.
Krivova, N.A., Solanki, S.K., Unruh, Y.C., 2011. Towards a long-term record of solar total and spectral irradiance. J. Atmos. Sol. Terr. Phys. 73 (2), 223–234. https://doi.org/10.1016/j.jastp.2009.11.013. ISSN 1364-6826.
Kuhnert, Henning, Kuhlmann, Holger, Mohtadi, Mahyar, Meggers, Helge, Baumann, Karl-Heinz, Pätzold, Jürgen, 2014. Holocene tropical western Indian Ocean sea surface temperatures in covariation with climatic changes in the Indonesian region. Paleoceanography 29 (5), 423–437. https://doi.org/10.1002/2013PA002555.
Lachniet, Matthew S., Denniston, Rhawn F., Asmerom, Yemane, Polyak, Victor J., 2014. Orbital control of western North America atmospheric circulation and climate over two glacial cycles. Nat. Commun. 5 (1), 3805. https://doi.org/10.1038/ncomms4805. ISSN 2041-1723.
Laepple, Thomas, Huybers, Peter, 2014a. Global and regional variability in marine surface temperatures. Geophys. Res. Lett. 41 (7), 2528–2534. https://doi.org/10.1002/2014GL059345. ISSN 0094-8276.
Laepple, Thomas, Huybers, Peter, 2014b. Ocean surface temperature variability: large model–data differences at decadal and longer periods. Proc. Natl. Acad. Sci. USA 111 (47), 16682–16687. https://doi.org/10.1073/pnas.1412077111.
Lamy, Frank, Rühlemann, Carsten, Hebbeln, Dierk, Wefer, Gerold, 2002. High- and low-latitude climate control on the position of the southern Peru-Chile Current during the Holocene. Paleoceanography 17 (2), 10–16. https://doi.org/10.1029/2001PA000727.
Lapointe, F., Bradley, R.S., Francus, P., Balascio, N.L., Abbott, M.B., Stoner, J.S., St-Onge, G., de Coninck, A., Labarre, T., 2020. Annually resolved Atlantic sea surface temperature variability over the past 2,900 y. Proc. Natl. Acad. Sci. U.S.A. 117 (44), 27171–27178. https://doi.org/10.1073/pnas.2014166117.
Larsen, Darren J., Miller, Gifford H., Geirsdóttir, Áslaug, Ólafsdóttir, Sædís, 2012. Non-linear Holocene climate evolution in the North Atlantic: a high-resolution, multi-proxy record of glacier activity and environmental change from Hvítárvatn, central Iceland. Quat. Sci. Rev. 39 (14–25). https://doi.org/10.1016/j.quascirev.2012.02.006. ISSN 0277-3791.
Lauritzen, Stein-Erik, Lundberg, Joyce, 1999. Calibration of the speleothem delta function: an absolute temperature record for the Holocene in northern Norway. Holocene 9 (6), 659–669. https://doi.org/10.1191/095968399667823929 https://doi.org/10.1191/095968399667823929.
Lee, J.-Y., Marotzke, J., Bala, G., Cao, L., Corti, S., Dunne, J.P., Engelbrecht, F., Fischer, E., Fyfe, J.C., Jones, C., Maycock, A., Mutemi, J., Ndiaye, O., Panickal, S., Zhou, T., 2021.

Future global climate: scenario-based projections and near- term information. In: Climate Change 2021: the Physical Science Basis. Contribution of Working Group I to the Sixth Assessment Report of the Intergovernmental Panel on Climate Change. Cambridge University Press, Cambridge, United Kingdom and New York, NY, USA, ISBN 9781009157896. https://doi.org/10.1017/9781009157896.006.553.

Linge, H., Lauritzen, S.-E., Andersson, C., Hansen, J.K., Skoglund, R.Ø., Sundqvist, H.S., 2009. Stable isotope records for the last 10 000 years from Okshola cave (Fauske, northern Norway) and regional comparisons. Clim. Past 5 (4), 667–682. https://doi.org/10.5194/cp-5-667-2009.

Linsley, Braddock K., Rosenthal, Yair, Oppo, Delia W., 2010. Holocene evolution of the Indonesian throughflow and the western Pacific warm pool. Nat. Geosci. 3 (8), 578–583. https://doi.org/10.1038/ngeo920. ISSN 1752-0908.

Litt, Thomas, Schölzel, Christian, Kühl, Norbert, Brauer, Achim, 2009. Vegetation and climate history in the Westeifel Volcanic Field (Germany) during the past 11 000 years based on annually laminated lacustrine maar sediments. Boreas 38 (4), 679–690. https://doi.org/10.1111/j.1502-3885.2009.00096.x.

Ljungqvist, Fredrik Charpentier, Zhang, Qiong, Brattström, Gudrun, Krusic, Paul J., Andrea Seim, Li, Qiang, Zhang, Qiang, Moberg, Anders, 2019. Centennial-scale temperature change in last millennium simulations and proxy-based reconstructions. J. Clim. 32 (9), 2441–2482. https://doi.org/10.1175/JCLI-D-18-0525.1.

Lohmann, Garrith, 2018. ESD Ideas: the stochastic climate model shows that underestimated Holocene trends and variability represent two sides of the same coin. Earth System Dynamics 9 (4), 1279–1281. https://doi.org/10.5194/esd-9-1279-2018.

Lundeen, Zachary, Brunelle, Andrea, Burns, Stephen J., Polyak, Victor, Asmerom, Yemane, 2013. A speleothem record of Holocene paleoclimate from the northern Wasatch Mountains, southeast Idaho, USA. Quat. Int. 310 (83–95). https://doi.org/10.1016/j.quaint.2013.03.018. ISSN 1040-6182.

Lüthi, Dieter, Le Floch, Martine, Bereiter, Bernhard, Blunier, Thomas, Barnola, Jean-Marc, Siegenthaler, Urs, Raynaud, Dominique, Jean, Jouzel, Fischer, Hubertus, Kawamura, Kenji, Stocker, Thomas F., 2008. High-resolution carbon dioxide concentration record 650,000–800,000 years before present. Nature 453 (7193), 379–382. https://doi.org/10.1038/nature06949. ISSN 1476-4687.

Mann, M.E., 2002. Climate reconstruction: the value of multiple proxies. Science 297 (5586), 1481–1482. https://doi.org/10.1126/science.1074318.

Mann, Michael E., Steinman, Byron A., Brouillette, Daniel J., Miller Sonya, K., 2021. Multidecadal climate oscillations during the past millennium driven by volcanic forcing. Science 371 (6533), 1014–1019. https://doi.org/10.1126/science.abc5810.

Marchitto, Thomas M., Muscheler, Raimund, Ortiz, Joseph D., Carriquiry, Jose D., Alexander van Geen, 2010. Dynamical response of the tropical pacific ocean to solar forcing during the early holocene. Science 330 (6009), 1378–1381. https://doi.org/10.1126/science.1194887.

Marsicek, Jeremiah, Shuman, Bryan N., Bartlein, Patrick J., Shafer, Sarah L., Brewer, Simon, 2018. Reconciling divergent trends and millennial variations in Holocene temperatures. Nature 554 (7690), 92–96. https://doi.org/10.1038/nature25464. ISSN 1476-4687.

Martin-Chivelet, Javier, María Muñoz-García, R Edwards, Turrero, María, Ortega, Ana, 2011. Land Surface temperature changes in Northern Iberia since 4000 yr BP, based on 13C of speleothemes. Global Planet. Change 77, 1–12. https://doi.org/10.1016/j.gloplacha.2011.02.002.

Mauritsen, Thorsten, Bader, Jürgen, Becker, Tobias, Behrens, Jörg, Bittner, Matthias, Brokopf, Renate, Brovkin, Victor, Martin, Claussen, Crueger, Traute, Esch, Monika, Fast, Irina, Fiedler, Stephanie, Fläschner, Dagmar, Gayler, Veronika, Giorgetta, Marco, Goll, Daniel S., Haak, Helmuth, Hagemann, Stefan, Hedemann, Christopher, Hohenegger, Cathy, Ilyina, Tatiana, Jahns, Thomas, Jimenéz-de-la Cuesta, Diego, Jungclaus, Johann, Kleinen, Thomas, Kloster, Silvia, Kracher, Daniela, Kinne, Stefan, Kleberg, Deike, Lasslop, Gitta, Kornblueh, Luis, Marotzke, Jochem, Daniela Matei, Meraner, Katharina, Mikolajewicz, Uwe, Modali, Kameswarrao, Möbis, Benjamin, Müller, Wolfgang A., Julia, E M S Nabel, Nam, Christine C.W., Notz, Dirk, Nyawira, Sarah-Sylvia, Hanna, Paulsen, Peters, Karsten, Pincus, Robert, Pohlmann, Holger, Julia, Pongratz, Popp, Max, Raddatz, Thomas Jürgen, Rast, Sebastian, Redler, Rene, Reick, Christian H., Tim Rohrschneider, Vera, Schemann, Schmidt, Hauke, Schnur, Reiner, Schulzweida, Uwe, Katharina, D Six, Stein, Lukas, Irene Stemmler, Stevens, Bjorn, von Storch, Jin-Song, Tian, Fangxing, Voigt, Aiko, Vrese, Philipp, Wieners, Karl-Hermann, Wilkenskjeld, Stiig, Winkler, Alexander, Roeckner, Erich, 2019. Developments in the MPI-M earth system Model version 1.2 (MPI-ESM1.2) and its Response to increasing CO2. J. Adv. Model. Earth Syst. 11 (4), 998–1038. https://doi.org/10.1029/2018MS001400.

McAndrews, John H., 1984. Pollen analysis of the 1973 ice core from Devon Island glacier, Canada. Quat. Res. 22 (1), 68–76. https://doi.org/10.1016/0033-5894(84)90007-3. ISSN 0033-5894.

McClymont, Erin L., Ganeshram, Raja S., Pichevin, Laetitia E., Talbot, Helen M., Dongen, Bart E van, Thunell, Robert C., Haywood, Alan M., Singarayer, Joy S., Valdes, Paul J., 2012. Sea-surface temperature records of Termination 1 in the Gulf of California: challenges for seasonal and interannual analogues of tropical Pacific climate change. Paleoceanography 27 (2). https://doi.org/10.1029/2011PA002226.

McDermott, Frank, Mattey, David P., Hawkesworth, Chris, 2001. *Centennial-scale holocene climate variability Revealed by a high-resolution speleothem $\delta^{18}O$ Record from SW Ireland*. Science 294 (5545), 1328–1331. ISSN 00368075, 10959203.

McKay, Nicholas, Kaufman, Darrell, 2009. Holocene climate and glacier variability at hallet and greyling lakes, chugach mountains, south-central Alaska. J. Paleolimnol. 41, 143–159. https://doi.org/10.1007/s10933-008-9260-0.

McKay, Nicholas P., Kaufman, Darrell S., 2014. An extended Arctic proxy temperature database for the past 2,000 years. Sci. Data 1 (1), 140026. https://doi.org/10.1038/sdata.2014.26. ISSN 2052-4463.

Mezgec, K., Stenni, B., Crosta, X., Masson-Delmotte, V., Baroni, C., Braida, M., Ciardini, V., Colizza, E., Melis, R., Salvatore, M.C., Severi, M., Scarchilli, C., Traversi, R., Udisti, R., Frezzotti, M., 2017. Holocene sea ice variability driven by wind and polynya efficiency in the Ross Sea. Nat. Commun. 8 (1), 1334. https://doi.org/10.1038/s41467-017-01455-x. ISSN 2041-1723.

Minoshima, Kayo, Kawahata, Hodaka, Ikehara, Ken, 2007. Changes in biological production in the mixed water region (MWR) of the northwestern North Pacific during the last 27 kyr. Palaeogeogr. Palaeoclimatol. Palaeoecol. 254 (3), 430–447. https://doi.org/10.1016/j.palaeo.2007.06.022. ISSN 0031-0182.

Mohtadi, Mahyar, Prange, Matthias, Oppo, Delia W., De Pol-Holz, Ricardo, Merkel, Ute, Zhang, Xiao, Stephan Steinke, Lückge, Andreas, 2014. North Atlantic forcing of tropical Indian Ocean climate. Nature 509 (7498), 76–80. https://doi.org/10.1038/nature13196. ISSN 1476-4687.

Mosley-Thompson, Ellen, 1996. Climatic Variations and Forcing Mechanisms of the Last 2000 Years. Holocene Climate Changes Recorded in an East Antarctica Ice Core. Springer Berlin Heidelberg, Berlin, Heidelberg, ISBN 978-3-642-61113-1.

Mudelsee, Manfred, 2002. TAUEST: a computer program for estimating persistence in unevenly spaced weather/climate time series. Comput. Geosci. 28, 69–72. https://doi.org/10.1016/S0098-3004(01)00041-3.

Müller, Juliane, Werner, Kirstin, Stein, Ruediger, Fahl, Kirsten, Moros, Matthias, Jansen, Eystein, 2012. Holocene cooling culminates in Neoglacial sea ice oscillations in Fram Strait. Quat. Sci. Rev. 47 (1–14). https://doi.org/10.1016/j.quascirev.2012.04.024.

NCAR, 2011. TraCE-21ka: Simulation of Transient Climate Evolution over the Last 21,000 Years. https://www.cgd.ucar.edu/ccr/TraCE/. Accessed: 23-04-2022.

Neil, Karen, Gajewski, Konrad, Betts, Matthew, 2014. Human-ecosystem interactions in relation to holocene environmental change in port joli harbour, southwestern nova scotia, Canada. Quat. Res. 81 (2), 203–212. https://doi.org/10.1016/j.yqres.2014.01.001. ISSN 0033-5894.

Nichols, Harvey, 1975. Palynological and Paleoclimatic Study of the Late Quaternary Displacement of the Boreal Forest-Tundra Ecotone in Keewatin and Mackenzie, NWT, vol. 15. *Canada*. University of Colorado, Institute of Arctic and Alpine Research, Occasional Paper.

Nielsen, Simon H.H., Koc, Nalan, Crosta, Xavier, 2004. Holocene climate in the Atlantic sector of the Southern Ocean: controlled by insolation or oceanic circulation? Geology 32 (4), 317–320. https://doi.org/10.1130/G20334.1. ISSN 0091-7613.

Ogurtsov, M.G., Nagovitsyn, YuA., Kocharov, G.E., Jungner, H., 2002. Long-period cycles of the sun's activity recorded in direct solar data and proxies. Sol. Phys. 211 (1), 371–394. https://doi.org/10.1023/A:1022411209257. ISSN 1573-093X.

Ojala, A.E.K., Alenius, T., Seppä, H., Giesecke, T., 2008. Integrated varve and pollen-based temperature reconstruction from Finland: evidence for Holocene seasonal temperature patterns at high latitudes. Holocene 18 (4), 529–538. https://doi.org/10.1177/0959683608089207.

Olsen, Jesper, Björck, Svante, Melanie, J Leng, Gudmundsdóttir, Esther Ruth, Bent, V Odgaard, Lutz, Christina M., Kendrick, Chris P., Thorbjørn, J Andersen, Seidenkrantz, Marit-Solveig, 2010. Lacustrine evidence of Holocene environmental change from three Faroese lakes: a multiproxy XRF and stable isotope study. Quat. Sci. Rev. 29 (19), 2764–2780. https://doi.org/10.1016/j.quascirev.2010.06.029. ISSN 0277-3791.

Otto-Bliesner, B.L., Braconnot, P., Harrison, S.P., Lunt, D.J., Abe-Ouchi, A., Albani, S., Bartlein, P.J., Capron, E., Carlson, A.E., Dutton, A., Fischer, H., Goelzer, H., Govin, A., Haywood, A., Joos, F., LeGrande, A.N., Lipscomb, W.H., Lohmann, G., Mahowald, N., Nehrbass-Ahles, C., Pausata, F.S.R., Peterschmitt, J.-Y., Phipps, S.J., Renssen, H., Zhang, Q., 2017. The PMIP4 contribution to CMIP6 - Part 2: two interglacials, scientific objective and experimental design for Holocene and Last Interglacial simulations. Geosci. Model Dev. (GMD) 10 (11), 3979–4003. https://doi.org/10.5194/gmd-10-3979-2017.

Park, W., Latif, M., 2008. Multidecadal and multicentennial variability of the meridional overturning circulation. Geophys. Res. Lett. 35 (22). https://doi.org/10.1029/2008GL035779. ISSN 0094-8276.

Parsons, Luke A., Loope, Garrison R., Overpeck, Jonathan T., Ault, Toby R., Stouffer, Ronald, Cole, Julia E., 2017. Temperature and precipitation variance in CMIP5 simulations and paleoclimate records of the last millennium. J. Clim. 30 (22), 8885–8912. https://doi.org/10.1175/JCLI-D-16-0863.1.

Pelejero, Carles, Grimalt, Joan O., Heilig, Stephanie, Kienast, Markus, Wang, Luejiang, 1999. High-resolution UK 37 temperature reconstructions in the South China Sea over the past 220 kyr. Paleoceanography 14 (2), 224–231. https://doi.org/10.1029/1998PA900015.

Petersen, K.L., 1985. Palynology in Montezuma County, southwestern Colorado: the local history of pinyon pine (Pinus edulis). ASSP Contrib. Ser 16, 47–62.

Rao, Zhiguo, Huang, Chao, Xie, Luhua, Shi, Fuxi, Zhao, Yan, Cao, Jiantao, Gou, Xiaohua, Chen, Jianhui, Chen, Fahu, 2019. Long-term summer warming trend during the Holocene in central Asia indicated by alpine peat α-cellulose δ13C record. Quat. Sci. Rev. 203 (56–67). https://doi.org/10.1016/j.quascirev.2018.11.010. ISSN 0277-3791.

Rimbu, N., Lohmann, G., Lorenz, S.J., Kim, J.H., Schneider, R.R., 2004. Holocene climate variability as derived from alkenone sea surface temperature and coupled ocean-atmosphere model experiments. Clim. Dynam. 23 (2), 215–227.

https://doi.org/10.1007/s00382-004-0435-8. ISSN 1432-0894.
Risebrobakken, Bjørg, Jansen, Eystein, Dahl, Carin Andersson, Mjelde, Eirik, Hevrøy, Kjersti, 2003. A high-resolution study of Holocene paleoclimatic and paleoceanographic changes in the Nordic Seas. Paleoceanography 18. https://doi.org/10.1029/2002PA000764.
Rodrigues, Teresa, Grimalt, Joan O., Abrantes, Fátima, Naughton, Filipa, Flores, José-Abel, 2010. The last glacial–interglacial transition (LGIT) in the western mid-latitudes of the North Atlantic: abrupt sea surface temperature change and sea level implications. Quat. Sci. Rev. 29 (15), 1853–1862. https://doi.org/10.1016/j.quascirev.2010.04.004. ISSN 0277-3791.
Rösch, Manfred, 2009. Botanical Evidence for Prehistoric and Medieval Land Use in the Black Forest. Brepols Publishers, ISBN 978-2-503-52746-8. https://doi.org/10.1484/M.RURALIA-. EB.3.1181.
Rosenthal, Yair, Oppo, Delia W., Linsley, Braddock K., 2003. The amplitude and phasing of climate change during the last deglaciation in the Sulu Sea, western equatorial Pacific. Geophys. Res. Lett. 30 (8). https://doi.org/10.1029/2002GL016612.
Salzer, Matthew W., Bunn, Andrew G., Graham, Nicholas E., Hughes, Malcolm K., 2014. Five millennia of paleotemperature from tree-rings in the Great Basin, USA. Clim. Dynam. 42 (5), 1517–1526. https://doi.org/10.1007/s00382-013-1911-9. ISSN 1432-0894.
Sarnthein, M., Van Kreveld, S., Erlenkeuser, H., Grootes, P.M., Kucera, M., Pflaumann, U., Schulz, M., 2003. Centennial-to-millennial-scale periodicities of Holocene climate and sediment injections off the western Barents shelf, 75°N. Boreas 32 (3), 447–461. https://doi.org/10.1111/j.1502-3885.2003.tb01227.x.
Schmidt, Matthew W., Stieglitz, Jean Lynch, 2011. Florida Straits deglacial temperature and salinity change: implications for tropical hydrologic cycle variability during the Younger Dryas. Paleoceanography 26 (4). https://doi.org/10.1029/2011PA002157.
Schmidt, Matthew W., Weinlein, William A., Franco, Marcantonio, Lynch-Stieglitz, Jean, 2012. Solar forcing of Florida Straits surface salinity during the early Holocene. Paleoceanography 27 (3). https://doi.org/10.1029/2012PA002284. ISSN 0883-8305.
Schröder, Jan F., Holbourn, Ann, Kuhnt, Wolfgang, Küssner, Kevin, 2016. Variations in sea surface hydrology in the southern Makassar Strait over the past 26 kyr. Quat. Sci. Rev. 154 (143–156). https://doi.org/10.1016/j.quascirev.2016.10.018. ISSN 0277-3791.
Sejrup, H., Haflidason, Haflidi, Andrews, John, 2011. A Holocene North Atlantic SST record and regional climate variability. Quat. Sci. Rev. 30, 3181–3195. https://doi.org/10.1016/j.quascirev.2011.07.025.
Seppä, H., Bjune, A.E., Telford, R.J., Birks, H.J.B., Veski, S., 2009. Last nine-thousand years of temperature variability in Northern Europe. Clim. Past 5 (3), 523–535. https://doi.org/10.5194/cp-5-523-2009.
Sheather, S.J., Jones, M.C., 1991. A reliable data-based bandwidth selection method for kernel density estimation. J. Roy. Stat. Soc. B 53 (3), 683–690. https://doi.org/10.1111/j.2517-6161.1991.tb01857.x. ISSN 0035-9246.
Shi, Xiaoxu, Lohmann, Gerrit, Dmitry Sidorenko, Hu, Yang, 2020. Early-Holocene simulations using different forcings and resolutions in AWI-ESM. Holocene 30 (7), 996–1015. https://doi.org/10.1177/0959683620908634.
Shi, X., Werner, M., Krug, C., Brierley, C.M., Zhao, A., Igbinosa, E., Braconnot, P., Brady, E., Cao, J., D'Agostino, R., Jungclaus, J., Liu, X., Otto-Bliesner, B., Sidorenko, D., Tomas, R., Volodin, E.M., Yang, H., Zhang, Q., Zheng, W., Lohmann, G., 2021. Calendar effects on surface air temperature and precipitation based on model-ensemble equilibrium and transient simulations from PMIP4 and PACMEDY. Clim. Past Discuss 1–29, 2021. https://doi.org/10.5194/cp-2021-163.
Shotyk, W., Cheburkin, A.K., Appleby, P.G., Fankhauser, A., Kramers, J.D., 1997. Lead in three peat bog profiles, jura mountains, Switzerland: enrichment factors, isotopic composition, and chronology of atmospheric deposition. Water Air Soil Pollut. 100 (3), 297–310. https://doi.org/10.1023/A:1018384711802. ISSN 1573-2932.
Shuman, Bryan N., Marsicek, Jeremiah, 2016. The structure of Holocene climate change in mid-latitude North America. Quat. Sci. Rev. 141 (38–51). https://doi.org/10.1016/j.quascirev.2016.03.009. ISSN 0277-3791.
Sigl, M., Toohey, M., McConnell, J.R., Cole-Dai, J., Severi, M., 2022. Volcanic stratospheric sulfur injections and aerosol optical depth during the Holocene (past 11 500 years) from a bipolar ice-core array. Earth Syst. Sci. Data 14 (7), 3167–3196. https://doi.org/10.5194/essd-14-3167-2022.
Staubwasser, Michael, Frank, Sirocko, Grootes, Pieter M., Erlenkeuser, Helmut, 2002. South Asian monsoon climate change and radiocarbon in the Arabian Sea during early and middle Holocene. Paleoceanography 17 (4), 12–15. https://doi.org/10.1029/2000PA000608. ISSN 0883-8305.
Stefani, F., Stepanov, R., Weier, T., 2021. Shaken and stirred: when Bond meets suess–de Vries and gnevyshev–ohl. Sol. Phys. 296 (6), 88. https://doi.org/10.1007/s11207-021-01822-4. ISSN 1573-093X.
Stenni, B., Masson-Delmotte, V., Selmo, E., Oerter, H., Meyer, H., Röthlisberger, R., Jouzel, J., Cattani, O., Falourd, S., Fischer, H., Hoffmann, G., Iacumin, P., Johnsen, S.J., Minster, B., Udisti, R., 2010. The deuterium excess records of EPICA Dome C and Dronning Maud Land ice cores (East Antarctica). Quat. Sci. Rev. 29 (1), 146–159. https://doi.org/10.1016/j.quascirev.2009.10.009. ISSN 0277-3791.
Stott, Lowell, Timmermann, Axel, Thunell, Robert, 2007. Southern Hemisphere and deep-sea warming led deglacial atmospheric CO2</sub> Rise and tropical warming. Science 318 (5849), 435–438. https://doi.org/10.1126/science.1143791.
Stuiver, M., Grootes, P.M., Braziunas, T.F., 1995. The GISP2 δ18O climate record of the past 16,500 years and the role of the sun, ocean, and volcanoes. Quat. Res. 44 (3), 341–354. https://doi.org/10.1006/qres.1995.1079.
Sun, Weiyi, Liu, Jian, Wan, Lingfeng, Ning, Liang, Yan, Mi, 2020. Simulation of northern hemisphere mid-latitude precipitation response to different external forcings during the Holocene. Quat. Sci. 40 (6), 1588–1596. https://doi.org/10.11928/j.issn.1001-7410.2020.06.18. ISSN 1001-7410.
Sun, Weiyi, Liu, Jian, Wang, Bin, Chen, Deliang, Wan, Lingfeng, Wang, Jing, 2022. Holocene multi-centennial variations of the asian summer monsoon triggered by solar activity. Geophys. Res. Lett. 49 (13), e2022GL098625. https://doi.org/10.1029/2022GL098625. ISSN 0094-8276.
Sundqvist, H.S., Kaufman, D.S., McKay, N.P., Balascio, N.L., Briner, J.P., Cwynar, L.C., Sejrup, H.P., Seppä, H., Subetto, D.A., Andrews, J.T., Axford, Y., Bakke, J., Birks, H.J.B., Brooks, S.J., De Vernal, A., Jennings, A.E., Ljungqvist, F.C., Rühland, K.M., Saenger, C., Smol, J.P., Viau, A.E., 2014. Arctic Holocene proxy climate database; New approaches to assessing geochronological accuracy and encoding climate variables. Clim. Past 10 (4), 1605–1631. https://doi.org/10.5194/cp-10-1605-2014. URL. https://www.ncei.noaa.gov/access/paleo-search/study/15444. (Accessed 3 November 2021). Accessed.
Taricco, C., Mancuso, S., Ljungqvist, F.C., Alessio, S., Ghil, M., 2015. Multispectral analysis of Northern Hemisphere temperature records over the last five millennia. Clim. Dynam. 45 (1), 83–104. https://doi.org/10.1007/s00382-014-2331-1. ISSN 1432-0894.
Usoskin, I.G., Gallet, Y., Lopes, F., Kovaltsov, G.A., Hulot, G., 2016. Solar activity during the Holocene: the Hallstatt cycle and its consequence for grand minima and maxima. Astron. Astrophys. 587, A150. https://doi.org/10.1051/0004-6361/201527295. ISSN 0004-6361.
van der Bilt, Willem G.M., D'Andrea, William J., Bakke, Jostein, Balascio, Nicholas L., Werner, Johannes P., Gjerde, Marthe, Bradley, Raymond S., 2018. Alkenone-based reconstructions reveal four-phase Holocene temperature evolution for High Arctic Svalbard. Quat. Sci. Rev. 183, 204–213. https://doi.org/10.1016/j.quascirev.2016.10.006. ISSN 0277-3791.
Vare, Lindsay L., Massé, Guillaume, Gregory, Thomas R., Smart, Christopher W., Simon, T., 2009. Belt. *Sea ice variations in the central Canadian arctic Archipelago during the holocene*. Quat. Sci. Rev. 28 (13–14), 1354–1366. https://doi.org/10.1016/j.quascirev.2009.01.013.
Vasskog, Kristian, Paasche, Øyvind, Nesje, Atle, Boyle, John F., Birks, H.J.B., 2012. A new approach for reconstructing glacier variability based on lake sediments recording input from more than one glacier. Quat. Res. 77 (1), 192–204. https://doi.org/10.1016/j.yqres.2011.10.001.
Vellinga, Michael, Wu, Peili, 2004. Low-latitude freshwater influence on centennial variability of the atlantic thermohaline circulation. J. Clim. 17 (23), 4498–4511. https://doi.org/10.1175/3219.1.
Veres, D., Bazin, L., Landais, A., Toyé Mahamadou Kele, H., Lemieux-Dudon, B., Parrenin, F., Martinerie, P., Blayo, E., Blunier, T., Capron, E., Chappellaz, J., Rasmussen, S.O., Severi, M., Svensson, A., Vinther, B., Wolff, E.W., 2013. The Antarctic ice core chronology (AICC2012): an optimized multi-parameter and multi-site dating approach for the last 120 thousand years. Clim. Past 9 (4), 1733–1748. https://doi.org/10.5194/cp-9-1733-2013.
Vieira, L.E.A., Solanki, S.K., Krivova, N.A., Usoskin, I., 2011. Evolution of the solar irradiance during the Holocene. A&A 531 (A6). https://doi.org/10.1051/0004-6361/201015843.
Vimeux, Françoise, Cuffey, Kurt M., Jean, Jouzel, 2002. New insights into Southern Hemisphere temperature changes from Vostok ice cores using deuterium excess correction. Earth Planet Sci. Lett. 203 (3), 829–843. https://doi.org/10.1016/S0012-821X(02)00950-0. ISSN 0012-821X.
Vinther, B.M., Clausen, H.B., Johnsen, S.J., Rasmussen, S.O., Andersen, K.K., Buchardt, S.L., Dahl-Jensen, D., Seierstad, I.K., Siggaard-Andersen, M.-L., Steffensen, J.P., Svensson, A., Olsen, J., Heinemeier, J., 2006. A synchronized dating of three Greenland ice cores throughout the Holocene. J. Geophys. Res. Atmos. 111 (D13). https://doi.org/10.1029/2005JD006921. ISSN 0148-0227.
Vinther, B.M., Buchardt, S.L., Clausen, H.B., Dahl-Jensen, D., Johnsen, S.J., Fisher, D.A., Koerner, R.M., Raynaud, D., Lipenkov, V., Andersen, K.K., Blunier, T., Rasmussen, S.O., Steffensen, J.P., Svensson, A.M., 2009. Holocene thinning of the Greenland ice sheet. Nature 461 (7262), 385–388. https://doi.org/10.1038/nature08355. ISSN 1476-4687.
Vorre, Karl-Dag, Jensen, Christin, Nilsen, Eilif, 2012. Climate changes during the last c. 7500 years as recorded by the degree of peat humification in the Lofoten region, Norway. Boreas 41. https://doi.org/10.1111/j.1502-3885.2011.00220.x.
Vorren, Karl-Dag, Blaauw, Maarten, Wastegaard, Stefan, Vander Plicht, Johannes, Jensen, Christin, 2007. High-resolution stratigraphy of the northernmost concentric raised bog in Europe: sellevollmyra, Andøya, northern Norway. Boreas 36 (3), 253–277. https://doi.org/10.1111/j.1502-3885.2007.tb01249.x.
Wanner, Heinz, Beer, Jürg, Bütikofer, Jonathan, Crowley, Thomas J., Ulrich, Cubasch, Flückiger, Jacqueline, Goosse, Hugues, Grosjean, Martin, Joos, Fortunat, Kaplan, Jed O., Küttel, Marcel, Müller, Simon A., Colin Prentice, I., Solomina, Olga, Stocker, Thomas F., Tarasov, Pavel, Wagner, Mayke, Martin, Widmann, 2008. Mid- to Late Holocene climate change: an overview. Quat. Sci. Rev. 27 (19), 1791–1828. https://doi.org/10.1016/j.quascirev.2008.06.013. ISSN 0277-3791.
Wanner, Heinz, Solomina, Olga, Grosjean, Martin, Ritz, Stefan P., Jetel, Markéta, 2011. Structure and origin of Holocene cold events. Quat. Sci. Rev. 30 (21), 3109–3123. https://doi.org/10.1016/j.quascirev.2011.07.010. ISSN 0277-3791.
Weldeab, Syee, Lea, David W., Schneider, Ralph R., Andersen, Nils, 2007. 155,000 Years of west african monsoon and ocean thermal evolution. Science 316 (5829), 1303–1307. https://doi.org/10.1126/science.1140461.

Wick, Lucia, Jacqueline Leeuwen, Knaap, Willem, Lotter, Andre, 2003. Holocene vegetation development in the catchment of S??gistalsee (1935 m asl), a small lake in the Swiss Alps. J. Paleolimnol. 30, 261–272. https://doi.org/10.1023/A:1026088914129.

Willemse, Nicolaas, Törnqvist, Torbjörn, 1999. Holocene century-scale temperature variability from West Greenland lake records. Geology 27 (580). https://doi.org/10.1130/0091-7613(1999)027¡0580:HCSTVF¿2.3.CO;2.

William D'Andrea, J., Huang, Yongsong, Fritz, Sherilyn C., Anderson, N John, 2011. Abrupt Holocene climate change as an important factor for human migration in West Greenland. Proc. Natl. Acad. Sci. USA 108 (24), 9765–9769. https://doi.org/10.1073/pnas.1101708108.

Williams, P.W., King, D.N.T., Zhao, J.-X., Collerson, K.D., 2005. Late Pleistocene to Holocene composite speleothem 18O and 13C chronologies from South Island, New Zealand—did a global Younger Dryas really exist? Earth Planet Sci. Lett. 230 (3), 301–317. https://doi.org/10.1016/j.epsl.2004.10.024. ISSN 0012-821X.

Wilson, I.R.G., 2013. The Venus–Earth–Jupiter spin–orbit coupling model. Pattern Recog. Phys. 1 (1), 147–158. https://doi.org/10.5194/prp-1-147-2013.

Wirtz, K.W., Lohmann, G., Bernhardt, K., Lemmen, C., 2010. Mid-Holocene regional reorganization of climate variability: analyses of proxy data in the frequency domain. Palaeogeogr. Palaeoclimatol. Palaeoecol. 298 (3), 189–200. https://doi.org/10.1016/j.palaeo.2010.09.019. ISSN 0031-0182.

Wu, C.J., Usoskin, I.G., Krivova, N., Kovaltsov, G.A., Baroni, M., Bard, E., Solanki, S.K., 2018. Solar activity over nine millennia: a consistent multi-proxy reconstruction. Astron. Astrophys. 615. https://doi.org/10.1051/0004-6361/201731892.

Li, Yang, Yang, Haijun, 2022. A theory for self-sustained multi-centennial oscillation of the atlantic meridional overturning circulation. J. Clim. https://doi.org/10.1175/JCLI-D-21-0685.1 pages 1–48.

Yin, Q.Z., Wu, Z.P., Berger, A., Goosse, H., Hodell, D., 2021. Insolation triggered abrupt weakening of Atlantic circulation at the end of interglacials. Science 373 (6558), 1035–1040. https://doi.org/10.1126/science.abg1737.

Yu, Shi-Yong, 2013. Quantitative reconstruction of mid- to late-Holocene climate in NE China from peat cellulose stable oxygen and carbon isotope records and mechanistic models. Holocene 23 (11), 1507–1516. https://doi.org/10.1177/0959683613496292.

Zatykó, Csilla, Juhász, Imola, Sümegi, 2007. Environmental Archaeology in Transdanubia. Varia Archaeologica Hungarica (20). Archaeological Institute of the Hungarian Academy of Sciences. ISBN 978-963-7391-94-1, Hardback.

Zhang, Q., Berntell, E., Axelsson, J., Chen, J., Han, Z., de Nooijer, W., Lu, Z., Li, Q., Zhang, Q., Wyser, K., Yang, S., 2021. Simulating the mid-Holocene, last interglacial and mid-Pliocene climate with EC-Earth3-LR. Geosci. Model Dev. (GMD) 14 (2), 1147–1169. https://doi.org/10.5194/gmd-14-1147-2021.

Zhao, Cheng, Liu, Zhonghui, Rohling, Eelco J., Yu, Zicheng, Liu, Weiguo, He, Yuxin, Zhao, Yan, Chen, Fahu, 2013. Holocene temperature fluctuations in the northern Tibetan Plateau. Quat. Res. 80 (1), 55–65. https://doi.org/10.1016/j.yqres.2013.05.001.

Zhu, Feng, Emile-Geay, Julien, McKay, Nicholas P., Hakim, Gregory J., Khider, Deborah, Ault, Toby R., Steig, Eric G., Dee, Sylvia, Kirchner, James W., 2019. Climate models can correctly simulate the continuum of global-average temperature variability. Proc. Natl. Acad. Sci. USA 116 (18), 8728–8733. https://doi.org/10.1073/pnas.1809959116.

Zielinski, Gregory A., Paul A Mayewski, L David Meeker, Whitlow, S., Mark S Twickler, A., 1996. 110,000-Yr record of explosive volcanism from the GISP2 (Greenland) ice core. Quat. Res. 45 (2), 109–118. https://doi.org/10.1006/qres.1996.0013. ISSN 0033-5894.